IEEE Access
Multidisciplinary | Rapid Review | Open Access Journal

Received 21 October 2023, accepted 7 November 2023, date of publication 14 November 2023, date of current version 20 November 2023.

Digital Object Identifier 10.1109/ACCESS.2023.3332656

RESEARCH ARTICLE

Multi-Stage Information Spreading Model in Simplicial Complexes Driven by Spatiotemporal Evolution of Public Health Emergency

YANYUAN SU[1,2,3], YAMING ZHANG[1,2,3], AND LI WEIGANG[4], (Senior Member, IEEE)

[1]School of Economics and Management, Yanshan University, Qinhuangdao 066004, China
[2]Research Center of Internet Plus and Industry Development, Yanshan University, Qinhuangdao 066004, China
[3]Research Center of Regional Economic Development, Yanshan University, Qinhuangdao 066004, China
[4]Department of Computer Science, University of Brasilia, Brasilia 70910-900, Brazil

Corresponding author: Yanyuan Su (suyanyuan1991@126.com)

This work was supported in part by the National Natural Science Foundation of China under Grant 72101227, in part by the Hebei Natural Science Foundation under Grant G2020203003, in part by the Science and Technology Research Project of Hebei Provincial Department of Education under Grant ZD2020199, and in part by the Hebei Xiong'an New Area Philosophy and Social Science Research Project under Grant XASK20221801.

ABSTRACT The long cycle and cross-region evolution of the public health emergency have caused sharp turbulence in the society. Especially, the multi-stage and multi-channel information spreading triggered by the public health emergency has further aggravated the social panic, and even caused a chain reaction to cause greater chaos. In this paper, we extend the information spreading to simplicial complexes, and analyze the effect of the spatiotemporal evolution of public health emergency on individuals' behaviors at each stage by taking 2-simplex as an example, firstly. Then the multi-stage information spreading dynamics model is constructed and the basic reproduction number is estimated. What's more, empirical analysis and simulation are carried out to verify the effectiveness and analyze the dynamics of the model. The results show that the strength effect of 2-simplex interactions would expand information's maximum impact, and enlarge the spreading scale. Besides, the information's impact and spreading scale at the first stage are positively correlated with epidemic's initial impact. The information could spread rapidly or even rebound and produce new peaks when the public health emergency getting worse. Especially, the rebound speed, peak and scale are negatively correlated with the initial impact of the public health emergency with epidemic local worsening. Moreover, the greater and the earlier of local and spatial deterioration, the greater the effect and the wider the information spreading scale. Furthermore, with the public health emergency in different regions getting worse or better in succession, the information's maximum impact and the spreading scale would be also enlarged. The results are useful to understand better the effect of public health emergency's spatiotemporal evolution on information spreading and suggest a promising way to weaken the negative effect of relevant information.

INDEX TERMS Information spreading, public health emergency, simplicial complexes, spatiotemporal evolution.

I. INTRODUCTION

The outbreak of public health emergency such as COVID-19, SARS, H5N1, H7N9, MERS and so on, often poses a serious threat to human health, triggers public panic, and inflicts a huge impact on the global economy and society [1], [2]. Especially, in the era of intelligent communication, individuals could express their opinions on multiple social networks in real time conveniently [3], [4], which leads to the emergence of relevant information immediately. While

The associate editor coordinating the review of this manuscript and approving it for publication was Hocine Cherifi.

the internet would also bring some disadvantages [5], [6]. For example, it could provide space for the spread of rumor and misinformation, and cause the flood of negative emotions as there are a lot of matters full of uncertainty or unknown after the outbreak of public health emergency [7], [8], [9], [10]. This will increase the risk of secondary derivative emergencies and chain reactions, challenge the governance and control ability of the government, and pose a serious threat to public security, social harmony and stability. Therefore, it is of great significance to study the complex information spreading process under public health emergencies.

At present, the research of information spreading has attracted extensive attention. Due to the similarity between information spreading and disease contagion, many scholars carried out the researches by establishing differential equations [11]. For example, based on the idea of Susceptible-Infected-Recovered (SIR) model [12], Daley and Kendall proposed D-K model, divided individuals' states into susceptible, infected and recovered, and constructed a dynamic model to solve the problem [13]. Subsequently, some scholars made some improvements by refining the spreading rules. For example, Maki and Thompson pointed out that the contact between two spreaders would promote the former to become recovered, and then proposed M-K model [14]. Besides, some researchers studied the problem from the perspective of ecosystem [15], and constructed mathematical model, like Lotka-Volterra and its improved models [16].

Since the 21st century, with the rapid development of information technology, public communication has become increasingly convenient. At the same time, information spreading is also increasingly affected by the structure of social networks [17]. Therefore, some scholars integrated the small-world [18], scale-free [19] and other characteristics of complex networks into the spreading model, and analyzed the spreading threshold and the stabilities of the equilibrium points. Zanette studied the dynamics of rumor spreading on small-world networks [20]. Moreno et al. analyzed the spreading process in complex heterogeneous networks [21]. Nekovee et al. found that the spreading threshold in scale-free network is small, and rumor is more likely to spread in scale-free networks [22]. Zhang et al. divided the spreader into independent spreader and cross network spreader, and proposed cross-network information spreading model in coupled networks [23]. Chai et al. considered the population disturbance and connectivity changes, proposed a stochastic information spreading model in complex social networks [24]. Dong et al. established an improved two-layer model to describe the dynamic process of rumor spreading in multiple channels [25]. Han et al. proposed a repeated rumor spreading model in coupled social networks [26]. Jing et al. proposed a spreading pairwise model on weighted networks to investigate the effects of weight distribution on rumor spreading [27]. Shao et al. developed a multilayer network spreading model by considering the coupling effect of online and offline communication [28].

In addition, because of the differences between information spreading and disease contagion, scholars also analyzed the spreading process considering the social attributes of the public in further [29]. Zhu and He considered the mobility of the crowd and studied rumor spreading based on reaction-diffusion model [30]. Ai et al. analyzed the impact of public anxiety on rumor spreading [31]. Cheng et al. considered the interaction between media and social networks, as well as factors such as delay and cost in the spreading process, and established a new delay model to analyze the dynamics of rumor spreading [32]. Wang et al. analyzed the differences in spreading behaviors among the individuals with different levels of scientific knowledge, and proposed a spreading dynamic model [33]. Suo et al. analyzed the information spreading process in complex social networks under different spreading strategies [34]. Yin et al. analyzed multi-topic discussion behavior under major public health events, and proposed a multiple-information susceptible-discussing-immune model to describe the multiple information spreading process [35]. Wang et al. proposed a novel model for the propagation of two rumors with mutual promotion [36]. Liu et al. proposed a rumor spreading dynamics model by incorporating the role of memory, user's ability to distinguish the rumors and rumor-denier's behavior of refuting rumors [37]. Yin et al. divided spreaders into super-infected and normal-infected according to the difference of their confidence in the rumor, and incorporated vigilantes and rumor de-bunkers to describe the diversity of information [38]. Zhang and Xu presented a model based on biomathematics theory to describe the interplay between rumors and rumor refutations [39]. Zhao et al. constructed a novel information spreading model considering the important role of opinion leaders and individuals' interest [40]. Li et al. simultaneously considered individual activity differences and rumor-refuting nodes, and proposed a new multifactor model to better analyze the process of rumor spreading in practice [41].

To some extent, scholars have conducted a series of researches on the information spreading mechanism based on disease dynamics and complex network theory. However, most of them only focused on the pairwise interactions and ignored the high-order interactions among individuals. Nowadays, more and more recent researches show that the high-order structures exist widely in the complex social networks and play an important role during spreading process, resulting in bistability, hysteresis, and explosive transitions [42], [43], [44]. Fan et al. found that 2-simplex could provide extra possibility for an individual to be informed [45]. Matamalas et al. analyzed the fixed-point solutions of the model, and found an interesting phase transition that became abrupt with the infectivity parameter of the 2-simplices [46]. Li et al. found that once the pairwise interactions gain coverage, high-order simplices would take

over and drive the spreading dynamics [47]. Gao et al. found that a canonical reaction-diffusion system defined over a simplicial complex would yield Turing patterns [48]. As these phenomena cannot be described simply by pairwise interactions, Iacopini et al. proposed a high-order model of social contagion in which a social system was represented by a simplicial complex and contagion could occur through interactions in groups of different sizes [49]. Jhun adopted hypergraph to describe high-order interactions between more than two individuals [50].

The above findings provide important references for analyzing the process of information spreading under public health emergencies. While most of them analyzed the process of information spreading under general cases. Although some scholars have studied the information spreading under natural disasters, social security and other emergencies, they usually took the emergency as static environment and did not consider enough the impact of the attributes and evolution characteristics of the emergencies. Therefore, the above researches might not be well applied to the analysis of information spreading driven by the dynamic evolution of public health emergencies. In 2015, Morgeson et al. proposed event system theory, pointed out that event intensity, duration and spatial diffusion could influence individuals' behaviors [51]. As we all know, except for the larger influence, public health emergencies also have some other characteristics like long-term and spatial diffusion. For example, the COVID-19 public health emergency has affected all regions of the world and has been assessed as a ''public health emergency of international concern'' by the World Health Organization (WHO), constituting a ''global pandemic''. In particular, affected by the evolution of public health emergency, relevant information emerges in stages [52]. Meanwhile, individuals usually show different spreading intentions according to whether the public health emergency occurred in the locality. That is to say, individuals usually have stronger intentions to spread public health emergency information if they are in the affected areas. Besides, the spreading intentions would change dynamically with the evolution of public health emergency [53]. Hence, the traditional SIR spreading model and the improved models such as Susceptible-Infected-Recovered-Susceptible (SIRS) have certain limitations due to insufficient consideration of the effect of public health emergency evolution and the heterogeneity of individuals' behaviors.

Inspired by the aforementioned analysis, we propose a novel $S_1S_2I_1I_2R$ model (S_1: susceptible in affected areas, S_2: susceptible in not affected areas, I_1: spreader in affected areas, I_2: spreader in not affected areas, R: recovered) to investigate multi-stage information spreading dynamics in simplicial complexes driven by the spatiotemporal evolution of public health emergency. As the main contributions of this paper, on the one hand, not only the pairwise information spreading is considered, but the group interactions are also integrated into the model. On the other hand, the effect of the dynamic evolution of public health emergency on the individuals' behaviors in different stages and states is analyzed. The mean-field equations are derived to describe the process of information spreading and the basic reproduction number is estimated. The results show that the strength effect of group interactions would expand information's maximum impact, and enlarge the spreading scale, but the inhibition effect would play the opposite role. Besides, we find that during the two-stage spreading process, the information's impact and spreading scale at the first stage are positively correlated with epidemic's initial impact, but are negatively correlated with initial impact as public health emergency local worsening. Especially, the relevant information may rebound to a new peak as public health emergency worsening. Moreover, the faster and greater the deterioration of public health emergency, the more serious the impact of information. It is helpful to understand better the mechanism and law of the multi-stage information spreading.

The remaining paper is organized as follows. In Section II, we analyze the effect of the dynamic evolution of public health emergency on the individuals' behaviors in different stages and states based on simplicial complexes. Then a novel $S_1S_2I_1I_2R$ model is introduced, and the mean-field equations are derived to describe the dynamics and the basic reproduction number is estimated in Section III. In Section IV, we present the simulations to verify the effectiveness of $S_1S_2I_1I_2R$ model and analyze the dynamics of the model. Finally, the conclusions are given in Section V.

II. EFFECT OF THE EVOLUTION OF PUBLIC HEALTH EMERGENCY IN SIMPLICIAL COMPLEXES

In this section, we introduce individuals' states during the information spreading process considering the regional differences and group interactions. Then, we describe the initial transition probabilities between different states in simplicial complexes. Moreover, the effect of evolution of public health emergency on transition probabilities are analyzed in further.

A. INDIVIDUAL STATES

In the existing researches about information spreading, individuals' states usually include three categories, namely susceptible (S), spreader (I), and recovered (R). Here, the susceptible (S) refers to the individual who has not spread public health emergency information but is very susceptible, the spreader (I) refers to the individual who is spreading public health emergency information, and the recovered (R) refers to the individual who is not interested in public health emergency information and does not spread it. However, since different individuals are in different situations, there are obvious regional differences for the spreading of public health emergency information in the network. Generally speaking, individuals in the areas affected by public health emergency are more likely to resonate with relevant topics, and pay more attention to the relevant information. This will enable local individuals to gather in the network, and then promote the rapid spread of public health emergency

information in a certain region. Therefore, in this paper, the susceptibles and spreaders are divided into two categories by taking account of the different behaviors of individuals in different regions when facing public health emergency. Besides, as recovereds do not spread the public health emergency information forever, they are not subdivided for simplicity. Hence, the individuals' states can be divided into the following five categories.

1) Susceptible in affected areas (S_1): individuals who are in the areas affected by public health emergency, and have not spread the information, but could be affected easily.
2) Spreader in affected areas (I_1): individuals who are in the areas affected by public health emergency, and are spreading the information.
3) Susceptible in not affected areas (S_2): individuals who are not in the areas affected by public health emergency, and have not spread the information, but could be affected easily.
4) Spreader in not affected areas (I_2): individuals who are not in the areas affected by public health emergency, and are spreading the information.
5) Recovered (R): individuals who are not interested in the public health emergency information and do not spread it.

TABLE 1. Initial transition probabilities under public health emergency.

Probability	Description
α_1	Probability that a susceptible in affected areas becomes a spreader in affected areas after receiving public health emergency information through pairwise interaction
β_1	Probability that a susceptible in affected areas becomes a recovered after receiving public health emergency information through pairwise interaction
α_1^Δ	Probability that a susceptible in affected areas becomes a spreader in affected areas after receiving public health emergency information through 2-simplex interactions
β_1^Δ	Probability that a susceptible in affected areas becomes a recovered after receiving public health emergency information through 2-simplex interactions
γ_1	Probability that a spreader in affected areas becomes a recovered
λ_1	Probability that a susceptible in not affected areas becomes a spreader in not affected areas after receiving public health emergency information through pairwise interaction
ξ_1	Probability that a susceptible in not affected areas becomes a recovered after receiving public health emergency information through pairwise interaction
λ_1^Δ	Probability that a susceptible in not affected areas becomes a spreader in not affected areas after receiving public health emergency information through 2-simplex interactions
ξ_1^Δ	Probability that a susceptible in not affected areas becomes a recovered after receiving public health emergency information through 2-simplex interactions
η_1	Probability that a spreader in not affected areas becomes a recovered

B. INITIAL TRANSITION PROBABILITIES IN SIMPLICIAL COMPLEXES

With public health emergency information spreading, individuals' states will exchange. Specifically, the susceptible would turn into the corresponding spreader after receiving the information, and the spreader might turn into the recovered. While it is worth noting that there are two ways for the susceptible to receive information in simplicial complexes. For simplicity, we just consider the 2-simplex here. On the one hand, the susceptible could receive the information through the direct neighbors who are spreading the information, namely pairwise interactions. On the other hand, the susceptible could also receive the information through simplicial complexes if the 2-simplex contains one susceptible and two spreaders, namely 2-simplex interactions.

Therefore, based on the definition method in Ref. [54], the initial transition probabilities could be set as Table 1. Here, the spreaders include both the spreaders in affected areas and those in not affected areas. Then the information spreading process with pairwise and 2-simplex interactions can be shown as Fig. 1. Obviously, α_1, β_1, α_1^Δ, β_1^Δ, γ_1, λ_1, ξ_1, λ_1^Δ, ξ_1^Δ, η_1 are all bounded in the interval [0,1] and satisfy $\alpha_1 + \beta_1 < 1$, $\lambda_1 + \xi_1 < 1$, $\alpha_1^\Delta + \beta_1^\Delta < 1$, $\lambda_1^\Delta + \xi_1^\Delta < 1$. Moreover, considering the difference of individuals' behaviors after receiving the public health emergency information, we assume that $\alpha_1 > \lambda_1$, $\beta_1 < \xi_1$, $\alpha_1^\Delta > \lambda_1^\Delta$, $\beta_1^\Delta < \xi_1^\Delta$, $\gamma_1 < \eta_1$. In addition, α_1, α_1^Δ, λ_1, λ_1^Δ describe the probability of susceptibles in affected areas and in not affected areas turning into the corresponding spreaders when receiving public health emergency information. That is to say, these four parameters reflect the initial impact of public health emergency on the individuals in different regions. For similarity, we set $\alpha_1^\Delta = \mu\alpha_1$, $\lambda_1^\Delta = \mu\lambda_1$, $\beta_1^\Delta = \sigma\beta_1$, $\xi_1^\Delta = \sigma\xi_1$. Here, μ shows the effect of 2-simplex interactions on susceptibles turning into the corresponding spreaders, and σ shows the effect of 2-simplex interactions on susceptibles turning into recovereds.

C. EFFECT OF EVOLUTION OF PUBLIC HEALTH EMERGENCY ON STATES TRANSITION

Different from general events, public health emergency like COVID-19 also has some special characteristics, such as long-period, multi-stage, spatial diffusion and so on. It is important to analyze the information spreading process considering the effect of the evolution of public health emergency. Here, the dynamic evolution of public health emergency includes not only the deterioration or improvement of emergency in affected areas, but also the interactive evolution between affected areas and not affected areas. Therefore, it is necessary to analyze the effect according to the changes at each stage and the spatial coverage of the affected areas. It is assumed that the evolution of public health emergency can be divided into n stages, $n \geq 1$.

On the one hand, the local deterioration or improvement degree of public health emergency in affected areas has an important effect on the transition probabilities. For clarity, the interactive evolution between affected areas and not affected areas is not considered. At stage n, each state transition

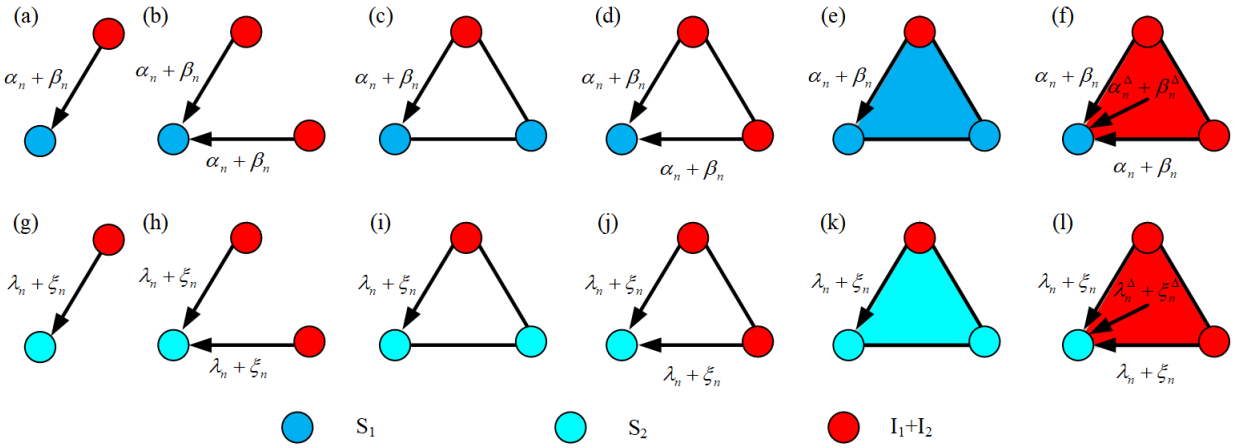

FIGURE 1. Different cases that susceptibles receiving public health emergency information with pairwise and 2-simplex interactions. (a)-(f) denote the different cases of susceptibles in affected areas, and (g)-(l) denote the different cases of susceptibles in not affected areas. (a) and (g) are cases of one 1-simplex (link) and the individual receives the public health emergency information from a spreader, then the individual would exchange the state with $\alpha_n + \beta_n$, $\lambda_n + \xi_n$ at each time step. (b) and (h) are cases of two 1-simplices, and the individual could receive the public health emergency information from two spreaders. (c), (d), (i) and (j) denote the cases of three 1-simplices as they do not form the 2-simplex since missing the face of the triangular enclosure. (e) and (k) denote the cases of one 2-simplex, but there is only one spreader in each of them, which does not meet the information spreading conditions of the 2-simplex. (f) and (l) denote the cases of one 2-simplex, and the susceptible not only could receive the public health emergency information through pairwise interactions and exchange the state with $\alpha_n + \beta_n$, $\lambda_n + \xi_n$, but also could receive the information through 2-simplex interactions and exchange the state with $\alpha_n^\Delta + \beta_n^\Delta$, $\lambda_n^\Delta + \xi_n^\Delta$.

probability in Table 1 can be expressed as α_n, β_n, α_n^Δ, β_n^Δ, γ_n, λ_n, ξ_n, λ_n^Δ, ξ_n^Δ, η_n, respectively. Compared with stage (n-1), the deterioration or improvement degree in affected areas at stage n is θ_n, and $\theta_n \geq 0, \theta_1 = 0$. Generally speaking, if public health emergency gets worse and worse, individuals would be more likely to be attracted by the relevant information, and keep spreading the information. This would result that the transition probability of susceptibles turning into spreaders increases rapidly to 1, and the probability of susceptibles or spreaders turning into recovereds decreases rapidly to 0. On the contrary, if public health emergency is well controlled, the attraction of relevant information will gradually decrease, and individuals tend to shift their attention to other things. This will result the probability of susceptibles turning into spreaders decreases rapidly to 0, and the probability of susceptibles or spreaders turning into recovereds increases rapidly to 1. In fact, the changes of transition probabilities are usually nonlinear with the evolution of public health emergency. In the existing researches, exponential function is often constructed to describe the nonlinear changing trend of transition probability [55]. Therefore, we use exponential function to describe the effect of public health emergency's local evolution in affected areas on transition probabilities. According to Ref. [56], when the public health emergency deteriorates locally at stage n ($n \geq 2$), the transition probabilities could be defined as

$$\begin{aligned}
\alpha_n &= 1 - (1 - \alpha_{n-1})e^{-\theta_n} \\
\beta_n &= \beta_{n-1}e^{-\theta_n} \\
\alpha_n^\Delta &= 1 - (1 - \alpha_{n-1}^\Delta)e^{-\theta_n} \\
\beta_n^\Delta &= \beta_{n-1}^\Delta e^{-\theta_n} \\
\gamma_n &= \gamma_{n-1}e^{-\theta_n} \\
\lambda_n &= 1 - (1 - \lambda_{n-1})e^{-\theta_n} \\
\xi_n &= \xi_{n-1}e^{-\theta_n} \\
\lambda_n^\Delta &= 1 - (1 - \lambda_{n-1}^\Delta)e^{-\theta_n} \\
\xi_n^\Delta &= \xi_{n-1}^\Delta e^{-\theta_n} \\
\eta_n &= \eta_{n-1}e^{-\theta_n}
\end{aligned} \tag{1}$$

While when the public health emergency gets better locally at stage n ($n \geq 2$), the transition probabilities could be defined as

$$\begin{aligned}
\alpha_n &= \alpha_{n-1}e^{-\theta_n} \\
\beta_n &= 1 - (1 - \beta_{n-1})e^{-\theta_n} \\
\alpha_n^\Delta &= \alpha_{n-1}^\Delta e^{-\theta_n} \\
\beta_n^\Delta &= 1 - (1 - \beta_{n-1}^\Delta)e^{-\theta_n} \\
\gamma_n &= 1 - (1 - \gamma_{n-1})e^{-\theta_n} \\
\lambda_n &= \lambda_{n-1}e^{-\theta_n} \\
\xi_n &= 1 - (1 - \xi_{n-1})e^{-\theta_n} \\
\lambda_n^\Delta &= \lambda_{n-1}^\Delta e^{-\theta_n} \\
\xi_n^\Delta &= 1 - (1 - \xi_{n-1}^\Delta)e^{-\theta_n} \\
\eta_n &= 1 - (1 - \eta_{n-1})e^{-\theta_n}
\end{aligned} \tag{2}$$

Obviously, α_n, β_n, α_n^Δ, β_n^Δ, γ_n, λ_n, ξ_n, λ_n^Δ, ξ_n^Δ, η_n are all bounded in the interval [0,1] and satisfy $\alpha_n + \beta_n < 1$, $\lambda_n + \xi_n < 1$, $\alpha_n^\Delta + \beta_n^\Delta < 1$, $\lambda_n^\Delta + \xi_n^\Delta < 1$.

On the other hand, the spatial diffusion and receding of public health emergency could lead to the interactive evolution between affected areas and not affected areas.

This would further result in the changes of individuals' states. Here, let δ_n denote the probability that affected area becomes not affected area, and let ε_n denote the probability that not affected area becomes affected area at stage n. Then the individuals' states would change with corresponding probabilities. When public health emergency spreads spatially at stage n, there would be more and more not affected areas turning into affected areas, i.e., $\delta_n < \varepsilon_n$. That means public health emergency deteriorates across affected areas and not affected areas in spatial dimension. On the contrary, when public health emergency is improved at stage n, there would be more and more affected areas turning into not affected areas, i.e., $\delta_n > \varepsilon_n$. It indicates that public health emergency gets better across affected areas and not affected areas in spatial dimension.

III. MULTI-STAGE SPREADING MODEL

In this section, we analyze information spreading process in simplicial complexes considering the spatiotemporal evolution of public health emergency. Then we derive mean-field equations to describe the dynamics of novel information spreading model called $S_1S_2I_1I_2R$. Besides, the basic reproduction number is also estimated. For simplicity, we just consider the 2-simplex here as above.

A. MODEL DESCRIPTION

According to the analysis of the effect caused by the evolution of public health emergency, information spreading rules in 2-simplex could be demonstrated as follows. Here, we take stage n as an example.

(1) When a susceptible in affected areas $S_{1(i)}$ receiving the public health emergency information sending by a spreader in affected areas $I_{1(j)}$ or not affected areas $I_{2(j)}$ through pairwise interaction, $S_{1(i)}$ may be eager to share the information to others and become a spreader in affected areas $I_{1(i)}$ with probability α_n. Besides, $S_{1(i)}$ may also think that the public health emergency information is inconsistent with the fact or not be interested in it and become a recovered $R_{(i)}$ with probability β_n. According to [57] and [58], the transitions can be denoted with Equation (3).

$$\begin{aligned} S_{1(i)} + I_{1(j)} &\xrightarrow{\alpha_n} I_{1(i)} + I_{1(j)} \\ S_{1(i)} + I_{2(j)} &\xrightarrow{\alpha_n} I_{1(i)} + I_{2(j)} \\ S_{1(i)} + I_{1(j)} &\xrightarrow{\beta_n} R_{(i)} + I_{1(j)} \\ S_{1(i)} + I_{2(j)} &\xrightarrow{\beta_n} R_{(i)} + I_{2(j)} \end{aligned} \tag{3}$$

(2) When a susceptible in affected areas $S_{1(i)}$ receiving the public health emergency information sending by two spreaders in affected areas $I_{1(j)}$, $I_{1(k)}$ or not affected areas $I_{2(j)}$, $I_{2(k)}$ through 2-simplex interactions, $S_{1(i)}$ might send the information to others and become a spreader in affected areas $I_{1(i)}$ with probability α_n^{Δ}. Besides, $S_{1(i)}$ might also doubt the authenticity of the public health emergency information or not be interested in it and become a recovered $R_{(i)}$ with probability β_n^{Δ}.Then the transitions can be denoted with Equation (4).

$$\begin{aligned} S_{1(i)} + I_{1(j)} + I_{1(k)} &\xrightarrow{\alpha_n^{\Delta}} I_{1(i)} + I_{1(j)} + I_{1(k)} \\ S_{1(i)} + I_{2(j)} + I_{1(k)} &\xrightarrow{\alpha_n^{\Delta}} I_{1(i)} + I_{2(j)} + I_{1(k)} \\ S_{1(i)} + I_{1(j)} + I_{2(k)} &\xrightarrow{\alpha_n^{\Delta}} I_{1(i)} + I_{1(j)} + I_{2(k)} \\ S_{1(i)} + I_{2(j)} + I_{2(k)} &\xrightarrow{\alpha_n^{\Delta}} I_{1(i)} + I_{2(j)} + I_{2(k)} \\ S_{1(i)} + I_{1(j)} + I_{1(k)} &\xrightarrow{\beta_n^{\Delta}} R_{(i)} + I_{1(j)} + I_{1(k)} \\ S_{1(i)} + I_{2(j)} + I_{1(k)} &\xrightarrow{\beta_n^{\Delta}} R_{(i)} + I_{2(j)} + I_{1(k)} \\ S_{1(i)} + I_{1(j)} + I_{2(k)} &\xrightarrow{\beta_n^{\Delta}} R_{(i)} + I_{1(j)} + I_{2(k)} \\ S_{1(i)} + I_{2(j)} + I_{2(k)} &\xrightarrow{\beta_n^{\Delta}} R_{(i)} + I_{2(j)} + I_{2(k)} \end{aligned} \tag{4}$$

(3) When a susceptible in not affected areas $S_{2(i)}$ receiving the public health emergency information sending by a spreader in affected areas $I_{1(j)}$ or not affected areas $I_{2(j)}$ through pairwise interaction, $S_{2(i)}$ might believe it and become a spreader in not affected areas $I_{2(i)}$ with probability λ_n. Besides, $S_{2(i)}$ may not be interested in it and become a recovered $R_{(i)}$ with probability ξ_n. Similarity, the transitions of $S_{2(i)}$ can be denoted with Equation (5).

$$\begin{aligned} S_{2(i)} + I_{1(j)} &\xrightarrow{\lambda_n} I_{2(i)} + I_{1(j)} \\ S_{2(i)} + I_{2(j)} &\xrightarrow{\lambda_n} I_{2(i)} + I_{2(j)} \\ S_{2(i)} + I_{1(j)} &\xrightarrow{\xi_n} R_{(i)} + I_{1(j)} \\ S_{2(i)} + I_{2(j)} &\xrightarrow{\xi_n} R_{(i)} + I_{2(j)} \end{aligned} \tag{5}$$

(4) When a susceptible in not affected areas $S_{2(i)}$ receiving the public health emergency information sending by two spreaders in affected areas $I_{1(j)}, I_{1(k)}$ or not affected areas $I_{2(j)}$, $I_{2(k)}$ through 2-simplex interactions, $S_{2(i)}$ might be inclined to share it and become a spreader in not affected areas $I_{2(i)}$ with probability λ_n^{Δ}. Besides, $S_{2(i)}$ may not be interested in it and become a recovered $R_{(i)}$ with probability ξ_n^{Δ}. Then the transitions of $S_{2(i)}$ can be denoted with Equation (6).

$$\begin{aligned} S_{2(i)} + I_{1(j)} + I_{1(k)} &\xrightarrow{\lambda_n^{\Delta}} I_{2(i)} + I_{1(j)} + I_{1(k)} \\ S_{2(i)} + I_{2(j)} + I_{1(k)} &\xrightarrow{\lambda_n^{\Delta}} I_{2(i)} + I_{2(j)} + I_{1(k)} \\ S_{2(i)} + I_{1(j)} + I_{2(k)} &\xrightarrow{\lambda_n^{\Delta}} I_{2(i)} + I_{1(j)} + I_{2(k)} \\ S_{2(i)} + I_{2(j)} + I_{2(k)} &\xrightarrow{\lambda_n^{\Delta}} I_{2(i)} + I_{2(j)} + I_{2(k)} \\ S_{2(i)} + I_{1(j)} + I_{1(k)} &\xrightarrow{\xi_n^{\Delta}} R_{(i)} + I_{1(j)} + I_{1(k)} \\ S_{2(i)} + I_{2(j)} + I_{1(k)} &\xrightarrow{\xi_n^{\Delta}} R_{(i)} + I_{2(j)} + I_{1(k)} \\ S_{2(i)} + I_{1(j)} + I_{2(k)} &\xrightarrow{\xi_n^{\Delta}} R_{(i)} + I_{1(j)} + I_{2(k)} \\ S_{2(i)} + I_{2(j)} + I_{2(k)} &\xrightarrow{\xi_n^{\Delta}} R_{(i)} + I_{2(j)} + I_{2(k)} \end{aligned} \tag{6}$$

(5) After a spreader in affected areas $I_{1(i)}$ spreading the public health emergency information to others, $I_{1(i)}$ may stop

spreading and become a recovered $R_{(i)}$ with probability γ_n. Then the transition of $I_{1(i)}$ can be expressed as

$$I_{1(i)} \xrightarrow{\gamma_n} R_{(i)} \tag{7}$$

(6) After a spreader in not affected areas $I_{2(i)}$ spreading the public health emergency information to others, $I_{2(i)}$ may stop spreading and become a recovered $R_{(i)}$ with probability η_n. Then the transition of $I_{2(i)}$ can be expressed as

$$I_{2(i)} \xrightarrow{\eta_n} R_{(i)} \tag{8}$$

(7) The spatial diffusion and receding of public health emergency could result in the interaction evolution between affected areas and not affected areas. Suppose that individual i is a susceptible in affected areas $S_{1(i)}$, individual j is a susceptible in not affected areas $S_{2(j)}$, individual k is a spreader in affected areas $I_{1(k)}$, and individual l is a spreader in not affected areas $I_{2(l)}$. With the effect of the spatial evolution of public health emergency, $S_{1(i)}$ turns into $S_{2(i)}$ with probability δ_n, $S_{2(j)}$ turns into $S_{1(j)}$ with probability ε_n, $I_{1(k)}$ turns into $I_{2(k)}$ with probability δ_n, and $I_{2(l)}$ turns into $I_{1(l)}$ with probability ε_n. Then the transitions can be described as

$$\begin{aligned} S_{1(i)} &\xrightarrow{\delta_n} S_{2(i)} \\ S_{2(j)} &\xrightarrow{\varepsilon_n} S_{1(j)} \\ I_{1(k)} &\xrightarrow{\delta_n} I_{2(k)} \\ I_{2(l)} &\xrightarrow{\varepsilon_n} I_{1(l)} \end{aligned} \tag{9}$$

According to the above spreading rules, the information spreading process at stage n driven by spatiotemporal evolution of public health emergency can be shown in Fig. 2.

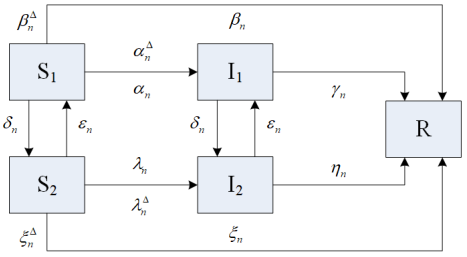

FIGURE 2. Process of information spreading in simplicial complexes under spatiotemporal evolution of public health emergency. α_n, β_n, λ_n, ξ_n are the state transition probabilities through pairwise interaction, α_n^Δ, β_n^Δ, λ_n^Δ, ξ_n^Δ are the state transition probabilities through 2-simplex interactions.

B. $S_1S_2I_1I_2R$ MODEL CONSIDERING SPATIOTEMPORAL EVOLUTION OF PUBLIC HEALTH EMERGENCY

Assuming individual i is a susceptible in affected areas $S_{1(i)}$ at time t, there are k adjacent nodes in the social network, among which g nodes are spreaders. Besides, the number of 2-simplices individual i belongs to is k^Δ. Among these 2-simplices, there are g^Δ 2-simplices including two spreaders. These spreaders will spread the public health emergency information in the time interval $[t, t+\Delta t]$. This will affect the individual i to change the state. We denote with $p^i_{S_1I_1}, p^i_{S_1R}$ the probability that individual i turns into a spreader in affected areas and a recovered respectively under the impact of the two categories or spreaders through pairwise and 2-simplex interactions. Then we can get

$$\begin{aligned} p^i_{S_1I_1} &= (1-(1-\alpha_n\Delta t)^g(1-\alpha_n^\Delta\Delta t)^{g^\Delta})(1-\delta_n\Delta t) \\ p^i_{S_1R} &= ((1-\alpha_n\Delta t)^g(1-\alpha_n^\Delta\Delta t)^{g^\Delta} - (1-(\alpha_n+\beta_n)\Delta t)^g \\ &\quad \times (1-(\alpha_n^\Delta+\beta_n^\Delta)\Delta t)^{g^\Delta})(1-\delta_n\Delta t) \end{aligned} \tag{10}$$

Here, g and g^Δ are random variables that satisfy the following distribution

$$\begin{aligned} \prod(g,t) &= \binom{k}{g} w(k,k^\Delta,t)^g(1-w(k,k^\Delta,t))^{k-g} \\ \prod(g^\Delta,t) &= \binom{k^\Delta}{g^\Delta} \varphi(k,k^\Delta,t)^{g^\Delta}(1-\varphi(k,k^\Delta,t))^{k^\Delta-g^\Delta} \end{aligned} \tag{11}$$

where $w(k,k^\Delta,t)$ is the probability at time t that an edge emanating from the individual with k neighbors and k^Δ 2-simplices points to a spreader in affected areas and not affected areas, and $\varphi(k,k^\Delta,t)$ is the probability at time t that the individual with k neighbors and k^Δ 2-simplices locates in a 2-simplex with two edges emanating from the individual pointing to two spreaders in affected areas and not affected areas, respectively. They can be written as

$$\begin{aligned} &w(k,k^\Delta,t) \\ &= \sum_{k',k^{\Delta'}} P(k',k^{\Delta'}|k,k^\Delta)(P(I_{1k'k^{\Delta'}}|S_{1kk^\Delta})+P(I_{2k'k^{\Delta'}}|S_{1kk^\Delta})) \\ &\approx \sum_{k',k^{\Delta'}} P(k',k^{\Delta'}|k,k^\Delta)(\rho^{I_1}(k',k^{\Delta'},t)+\rho^{I_2}(k',k^{\Delta'},t)) \\ &= \sum_{k',k^{\Delta'}} k'P(k',k^{\Delta'})(\rho^{I_1}(k',k^{\Delta'},t)+\rho^{I_2}(k',k^{\Delta'},t))\Big/\langle k\rangle \\ &= \sum_{k'} k'\Big/\langle k\rangle \sum_{k^{\Delta'}} P(k',k^{\Delta'})(\rho^{I_1}(k',k^{\Delta'},t)+\rho^{I_2}(k',k^{\Delta'},t)) \\ &= \sum_{k'} k'P(k')(\rho^{I_1}(k',t)+\rho^{I_2}(k',t))\Big/\langle k\rangle \\ &\varphi(k,k^\Delta,t) \\ &= \sum_{k',k^{\Delta'},k*,k^\Delta*} P(k',k^{\Delta'},k*,k^\Delta*|k,k^\Delta)(P(I_{1k'k^{\Delta'}}|S_{1kk^\Delta}) \\ &\quad + P(I_{2k'k^{\Delta'}}|S_{1kk^\Delta}))(P(I_{1k*k^\Delta*}|S_{1kk^\Delta}) \\ &\quad + P(I_{2k*k^\Delta*}|S_{1kk^\Delta})) \\ &\approx \sum_{k',k^{\Delta'},k*,k^\Delta*} P(k',k^{\Delta'},k*,k^\Delta*|k,k^\Delta)(\rho^{I_1}(k',k^{\Delta'},t) \\ &\quad + \rho^{I_2}(k',k^{\Delta'},t))(\rho^{I_1}(k*,k^\Delta*,t) \\ &\quad + \rho^{I_2}(k*,k^\Delta*,t)) \\ &= \sum_{k',k^{\Delta'},k*,k^\Delta*} k'P(k',k^{\Delta'})k*P(k*,k^\Delta*)(\rho^{I_1}(k',k^{\Delta'},t) \\ &\quad + \rho^{I_2}(k',k^{\Delta'},t))(\rho^{I_1}(k*,k^\Delta*,t) \end{aligned}$$

$$
\begin{aligned}
&+\rho^{I_2}(k*,k^{\Delta}*,t))\Big/\langle k\rangle^2\\
&=\sum_{k',k^{\Delta\prime}} k'P(k',k^{\Delta\prime})(\rho^{I_1}(k',k^{\Delta\prime},t)+\rho^{I_2}(k',k^{\Delta\prime},t))\Big/\langle k\rangle\\
&\quad\times\sum_{k*,k^{\Delta}*} k*P(k*,k^{\Delta}*)(\rho^{I_1}(k*,k^{\Delta}*,t)\\
&\quad+\rho^{I_2}(k*,k^{\Delta}*,t))\Big/\langle k\rangle\\
&=\sum_{k'} k'P(k')(\rho^{I_1}(k',t)+\rho^{I_2}(k',t))\Big/\langle k\rangle\\
&\quad\times\sum_{k*} k*P(k*)(\rho^{I_1}(k*,t)+\rho^{I_2}(k*,t))\Big/\langle k\rangle\\
&=\left[\sum_{k'} k'P(k')(\rho^{I_1}(k',t)+\rho^{I_2}(k',t))\Big/\langle k\rangle\right]^2 \qquad (12)
\end{aligned}
$$

In Equation (12), $P(k',k^{\Delta\prime}|k,k^{\Delta}) = k'P(k',k^{\Delta\prime})\Big/\langle k\rangle$ is the degree-degree correlation function, where $P(k,k^{\Delta})$ is the degree distribution and $\langle k\rangle$ is the average degree. $P(I_{1k'k^{\Delta\prime}}|S_{1kk^{\Delta}})$ and $P(I_{2k'k^{\Delta\prime}}|S_{1kk^{\Delta}})$ are the conditional probabilities that a spreader in affected areas or not affected areas with degree of 1-simplex k' and degree of 2-simplex $k^{\Delta\prime}$ is connected to a susceptible in affected areas with degree of 1-simplex k and degree of 2-simplex k^{Δ}, respectively. And $\rho^{I_1}(k',k^{\Delta\prime},t)$, $\rho^{I_2}(k',k^{\Delta\prime},t)$ are the densities of spreaders in affected areas or not affected areas at time t which belong to connectivity class $(k',k^{\Delta\prime})$, $\rho^{I_1}(k',t)$, $\rho^{I_2}(k',t)$ are the densities of spreaders in affected areas or not affected areas at time t which belong to connectivity class k', respectively. The approximations in Equation (12) are obtained by ignoring dynamic correlations between the states of neighboring individuals.

According to the above analysis, the transition probability $\bar{p}_{S_1I_1}(k,k^{\Delta},t)$ averaged over all possible values of g and g^{Δ} is given by

$$
\begin{aligned}
&\bar{p}_{S_1I_1}(k,k^{\Delta},t)\\
&=\sum_{g=0}^{k}\sum_{g^{\Delta}=0}^{k^{\Delta}}\binom{k}{g}w(k,k^{\Delta},t)^g(1-w(k,k^{\Delta},t))^{k-g}\\
&\quad\times\binom{k^{\Delta}}{g^{\Delta}}\varphi(k,k^{\Delta},t)^{g^{\Delta}}(1-\varphi(k,k^{\Delta},t))^{k^{\Delta}-g^{\Delta}}\\
&\quad\times(1-(1-\alpha_n\Delta t)^g(1-\alpha_n^{\Delta}\Delta t)^{g^{\Delta}})(1-\delta_n\Delta t)\\
&=(1-(1-\alpha_n w(k,k^{\Delta},t)\Delta t)^k(1-\alpha_n^{\Delta}\varphi(k,k^{\Delta},t)\Delta t)^{k^{\Delta}})\\
&\quad\times(1-\delta_n\Delta t) \qquad (13)
\end{aligned}
$$

Similarly, we can obtain

$$
\begin{aligned}
&\bar{p}_{S_1R}(k,k^{\Delta},t)\\
&=\sum_{g=0}^{k}\sum_{g^{\Delta}=0}^{k^{\Delta}}\binom{k}{g}w(k,k^{\Delta},t)^g(1-w(k,k^{\Delta},t))^{k-g}\\
&\quad\times\binom{k^{\Delta}}{g^{\Delta}}\varphi(k,k^{\Delta},t)^{g^{\Delta}}(1-\varphi(k,k^{\Delta},t))^{k^{\Delta}-g^{\Delta}}\\
&\quad\times((1-\alpha_n\Delta t)^g(1-\alpha_n^{\Delta}\Delta t)^{g^{\Delta}}-(1-(\alpha_n+\beta_n)\Delta t)^g\\
&\quad\times(1-(\alpha_n^{\Delta}+\beta_n^{\Delta})\Delta t)^{g^{\Delta}})(1-\delta_n\Delta t)\\
&=(1-\alpha_n w(k,k^{\Delta},t)\Delta t)^k(1-\alpha_n^{\Delta}\varphi(k,k^{\Delta},t)\Delta t)^{k^{\Delta}}\\
&\quad\times(1-\delta_n\Delta t)-(1-(\alpha_n+\beta_n)w(k,k^{\Delta},t)\Delta t)^k\\
&\quad\times(1-(\alpha_n^{\Delta}+\beta_n^{\Delta})\varphi(k,k^{\Delta},t)\Delta t)^{k^{\Delta}}(1-\delta_n\Delta t) \qquad (14)
\end{aligned}
$$

Following steps similar to the above, we can obtain other average transition probabilities of an individual with degree of 1-simplex k and degree of 2-simplex k^{Δ}

$$
\begin{aligned}
&\bar{p}_{S_2I_2}(k,k^{\Delta},t)\\
&=\sum_{g=0}^{k}\sum_{g^{\Delta}=0}^{k^{\Delta}}\binom{k}{g}w(k,k^{\Delta},t)^g(1-w(k,k^{\Delta},t))^{k-g}\\
&\quad\times\binom{k^{\Delta}}{g^{\Delta}}\varphi(k,k^{\Delta},t)^{g^{\Delta}}(1-\varphi(k,k^{\Delta},t))^{k^{\Delta}-g^{\Delta}}\\
&\quad\times(1-(1-\lambda_n\Delta t)^g(1-\lambda_n^{\Delta}\Delta t)^{g^{\Delta}})(1-\delta_n\Delta t)\\
&=(1-(1-\lambda_n w(k,k^{\Delta},t)\Delta t)^k(1-\lambda_n^{\Delta}\varphi(k,k^{\Delta},t)\Delta t)^{k^{\Delta}})\\
&\quad\times(1-\delta_n\Delta t) \qquad (15)\\
&\bar{p}_{S_2R}(k,k^{\Delta},t)\\
&=\sum_{g=0}^{k}\sum_{g^{\Delta}=0}^{k^{\Delta}}\binom{k}{g}w(k,k^{\Delta},t)^g(1-w(k,k^{\Delta},t))^{k-g}\\
&\quad\times\binom{k^{\Delta}}{g^{\Delta}}\varphi(k,k^{\Delta},t)^{g^{\Delta}}(1-\varphi(k,k^{\Delta},t))^{k^{\Delta}-g^{\Delta}}\\
&\quad\times((1-\lambda_n\Delta t)^g(1-\lambda_n^{\Delta}\Delta t)^{g^{\Delta}}-(1-(\lambda_n+\xi_n)\Delta t)^g\\
&\quad\times(1-(\lambda_n^{\Delta}+\xi_n^{\Delta})\Delta t)^{g^{\Delta}})(1-\delta_n\Delta t)\\
&=(1-\lambda_n w(k,k^{\Delta},t)\Delta t)^k(1-\lambda_n^{\Delta}\varphi(k,k^{\Delta},t)\Delta t)^{k^{\Delta}}\\
&\quad\times(1-\delta_n\Delta t)-(1-(\lambda_n+\xi_n)w(k,k^{\Delta},t)\Delta t)^k\\
&\quad\times(1-(\lambda_n^{\Delta}+\xi_n^{\Delta})\varphi(k,k^{\Delta},t)\Delta t)^{k^{\Delta}}(1-\delta_n\Delta t) \qquad (16)
\end{aligned}
$$

$$\bar{p}_{S_1S_2}(k,k^{\Delta},t)=\delta_n\Delta t \qquad (17)$$

$$\bar{p}_{S_2S_1}(k,k^{\Delta},t)=\varepsilon_n\Delta t \qquad (18)$$

$$\bar{p}_{I_1I_2}(k,k^{\Delta},t)=\delta_n\Delta t \qquad (19)$$

$$\bar{p}_{I_2I_1}(k,k^{\Delta},t)=\varepsilon_n\Delta t \qquad (20)$$

$$\bar{p}_{I_1R}(k,k^{\Delta},t)=\gamma_n\Delta t \qquad (21)$$

$$\bar{p}_{I_2R}(k,k^{\Delta},t)=\eta_n\Delta t \qquad (22)$$

Denote with $S_1(k,k^{\Delta},t)$, $S_2(k,k^{\Delta},t)$, $I_1(k,k^{\Delta},t)$, $I_2(k,k^{\Delta},t)$, $R(k,k^{\Delta},t)$ the expected values of the number of individuals belonging to connectivity class (k,k^{Δ}) which at time t are in state S_1, S_2, I_1, I_2 or R, respectively. Then the rate of change in the population of individuals in each state belonging to class (k,k^{Δ}) in the time interval $[t,t+\Delta t]$ could be given by

$$
\begin{aligned}
&S_1(k,k^{\Delta},t+\Delta t)\\
&=S_1(k,k^{\Delta},t)-S_1(k,k^{\Delta},t)\bar{p}_{S_1I_1}(k,k^{\Delta},t)\\
&\quad-S_1(k,k^{\Delta},t)\bar{p}_{S_1R}(k,k^{\Delta},t)
\end{aligned}
$$

$$
\begin{aligned}
&- S_1(k,k^{\Delta},t)\bar{p}_{S_1S_2}(k,k^{\Delta},t)\\
&+ S_2(k,k^{\Delta},t)\bar{p}_{S_2S_1}(k,k^{\Delta},t)\\
&S_2(k,k^{\Delta},t+\Delta t)\\
&= S_2(k,k^{\Delta},t) - S_2(k,k^{\Delta},t)\bar{p}_{S_2I_2}(k,k^{\Delta},t)\\
&- S_2(k,k^{\Delta},t)\bar{p}_{S_2R}(k,k^{\Delta},t)\\
&- S_2(k,k^{\Delta},t)\bar{p}_{S_2S_1}(k,k^{\Delta},t)\\
&+ S_1(k,k^{\Delta},t)\bar{p}_{S_1S_2}(k,k^{\Delta},t)\\
&I_1(k,k^{\Delta},t+\Delta t)\\
&= I_1(k,k^{\Delta},t) - I_1(k,k^{\Delta},t)\bar{p}_{I_1R}(k,k^{\Delta},t)\\
&- I_1(k,k^{\Delta},t)\bar{p}_{I_1I_2}(k,k^{\Delta},t) + S_1(k,k^{\Delta},t)\bar{p}_{S_1I_1}(k,k^{\Delta},t)\\
&+ I_2(k,k^{\Delta},t)\bar{p}_{I_2I_1}(k,k^{\Delta},t)\\
&I_2(k,k^{\Delta},t+\Delta t)\\
&= I_2(k,k^{\Delta},t) - I_2(k,k^{\Delta},t)\bar{p}_{I_2R}(k,k^{\Delta},t)\\
&- I_2(k,k^{\Delta},t)\bar{p}_{I_2I_1}(k,k^{\Delta},t) + S_2(k,k^{\Delta},t)\bar{p}_{S_2I_2}(k,k^{\Delta},t)\\
&+ I_1(k,k^{\Delta},t)\bar{p}_{I_1I_2}(k,k^{\Delta},t)\\
&R(k,k^{\Delta},t+\Delta t)\\
&= R(k,k^{\Delta},t) + S_1(k,k^{\Delta},t)\bar{p}_{S_1R}(k,k^{\Delta},t)\\
&+ S_2(k,k^{\Delta},t)\bar{p}_{S_2R}(k,k^{\Delta},t) + I_1(k,k^{\Delta},t)\bar{p}_{I_1R}(k,k^{\Delta},t)\\
&+ I_2(k,k^{\Delta},t)\bar{p}_{I_2R}(k,k^{\Delta},t) \qquad (23)
\end{aligned}
$$

Denote with $\rho^{S_1}(k,k^{\Delta},t)$, $\rho^{S_2}(k,k^{\Delta},t)$, $\rho^{I_1}(k,k^{\Delta},t)$, $\rho^{I_2}(k,k^{\Delta},t)$, $\rho^{R}(k,k^{\Delta},t)$ the fraction of individuals belonging to class (k,k^{Δ}) which are in state S_1, S_2, I_1, I_2, R, respectively. These quantities satisfy the normalization condition

$$
\begin{aligned}
\rho^{S_1}(k',k^{\Delta},t)+\rho^{S_2}(k',k^{\Delta},t)+\rho^{I_1}(k',k^{\Delta},t)+\rho^{I_2}(k',k^{\Delta},t)\\
+\rho^{R}(k',k^{\Delta},t)=1 \qquad (24)
\end{aligned}
$$

In the limit $\Delta t \to 0$, we can obtain the multi-stage information spreading dynamics model $S_1S_2I_1I_2R$ driven by the spatiotemporal evolution of public health emergency as follows

$$
\begin{aligned}
&\frac{\partial \rho^{S_1}(k,k^{\Delta},t)}{\partial t}\\
&= -k(\alpha_n+\beta_n)\rho^{S_1}(k,k^{\Delta},t)\sum_{k'}P(k'|k)(\rho^{I_1}(k',t)\\
&+\rho^{I_2}(k',t)) - k^{\Delta}(\alpha_n^{\Delta}+\beta_n^{\Delta})\rho^{S_1}(k,k^{\Delta},t)\\
&\times\left[\sum_{k'}P(k'|k)(\rho^{I_1}(k',t)+\rho^{I_2}(k',t))\right]^2\\
&-\delta_n\rho^{S_1}(k,k^{\Delta},t)+\varepsilon_n\rho^{S_2}(k,k^{\Delta},t)\\
&\frac{\partial \rho^{S_2}(k,k^{\Delta},t)}{\partial t}\\
&= -k(\lambda_n+\xi_n)\rho^{S_2}(k,k^{\Delta},t)\sum_{k'}P(k'|k)(\rho^{I_1}(k',t)\\
&+\rho^{I_2}(k',t)) - k^{\Delta}(\lambda_n^{\Delta}+\xi_n^{\Delta})\rho^{S_2}(k,k^{\Delta},t)\\
&\times\left[\sum_{k'}P(k'|k)(\rho^{I_1}(k',t)+\rho^{I_2}(k',t))\right]^2\\
&-\varepsilon_n\rho^{S_2}(k,k^{\Delta},t)+\delta_n\rho^{S_1}(k,k^{\Delta},t)\\
&\frac{\partial \rho^{I_1}(k,k^{\Delta},t)}{\partial t}\\
&= k\alpha_n\rho^{S_1}(k,k^{\Delta},t)\sum_{k'}P(k'|k)(\rho^{I_1}(k',t)+\rho^{I_2}(k',t))\\
&+k^{\Delta}\alpha_n^{\Delta}\rho^{S_1}(k,k^{\Delta},t)\\
&\times\left[\sum_{k'}P(k'|k)(\rho^{I_1}(k',t)+\rho^{I_2}(k',t))\right]^2\\
&-\delta_n\rho^{I_1}(k,k^{\Delta},t)+\varepsilon_n\rho^{I_2}(k,k^{\Delta},t)-\gamma_n\rho^{I_1}(k,k^{\Delta},t)\\
&\frac{\partial \rho^{I_2}(k,k^{\Delta},t)}{\partial t}\\
&= k\lambda_n\rho^{S_2}(k,k^{\Delta},t)\sum_{k'}P(k'|k)(\rho^{I_1}(k',t)+\rho^{I_2}(k',t))\\
&+k^{\Delta}\lambda_n^{\Delta}\rho^{S_2}(k,k^{\Delta},t)\\
&\times\left[\sum_{k'}P(k'|k)(\rho^{I_1}(k',t)+\rho^{I_2}(k',t))\right]^2\\
&-\varepsilon_n\rho^{I_2}(k,k^{\Delta},t)+\delta_n\rho^{I_1}(k,k^{\Delta},t)-\eta_n\rho^{I_2}(k,k^{\Delta},t)\\
&\frac{\partial \rho^{R}(k,k^{\Delta},t)}{\partial t}\\
&= k\beta_n\rho^{S_1}(k,k^{\Delta},t)\sum_{k'}P(k'|k)(\rho^{I_1}(k',t)+\rho^{I_2}(k',t))\\
&+k^{\Delta}\beta_n^{\Delta}\rho^{S_1}(k,k^{\Delta},t)\\
&\times\left[\sum_{k'}P(k'|k)(\rho^{I_1}(k',t)+\rho^{I_2}(k',t))\right]^2\\
&+k\xi_n\rho^{S_2}(k,k^{\Delta},t)\sum_{k'}P(k'|k)(\rho^{I_1}(k',t)+\rho^{I_2}(k',t))\\
&+k^{\Delta}\xi_n^{\Delta}\rho^{S_2}(k,k^{\Delta},t)\left[\sum_{k'}P(k'|k)(\rho^{I_1}(k',t)+\rho^{I_2}(k',t))\right]^2\\
&+\eta_n\rho^{I_2}(k,k^{\Delta},t)+\gamma_n\rho^{I_1}(k,k^{\Delta},t) \qquad (25)
\end{aligned}
$$

C. BASIC REPRODUCTION NUMBER

In the existing researches, the basic reproduction number R_0 is usually used as the judgment to estimate whether the information could spread in a large scale or not. Here, the basic reproduction number refers to the average number of individuals that can be affected by a new spreader under the situation that every individual is susceptible and without any external intervention. Therefore, we mainly analyze the spreading process of public health emergency information at the first stage. When the basic reproduction number $R_0 > 1$, the public health emergency information will spread in a large scale. However, when the basic reproduction number $R_0 < 1$, the public health emergency information could not spread widely.

We define $x = (I_1(t), I_2(t), R(t), S_1(t), S_2(t))^T$. Let $F(x)$ be the probability of appearance of new spreaders in each state, $V^+(x)$ be the probability of transition of individuals into each state by all other means, and $V^-(x)$ be the probability of

transition of individuals out of each state. Then we have $x' = F(x) - V(x)$, where $V(x) = V^-(x) - V^+(x)$. For simplicity, we set $w = w(k, k^\Delta, t)$, $\varphi = \varphi(k, k^\Delta, t)$. According to the model, when $n = 1$, we have (26) and (27), as shown at the bottom of the page.

Obviously, the system is stable when the public health emergency information does not exist and there are only two categories of susceptibles. Thus, we can verify that system has an equilibrium $E_0 = (0, 0, 0, S_1^*, S_2^*)$. According to Equation (25), $S_1^* = \varepsilon_1/(\delta_1 + \varepsilon_1)$, $S_2^* = \delta_1/(\delta_1 + \varepsilon_1)$. Then the derivatives $DF(E_0)$ and $DV(E_0)$ are partitioned as

$$DF(E_0) = \begin{bmatrix} F & 0 \\ 0 & 0 \end{bmatrix}, \quad DV(E_0) = \begin{bmatrix} V & 0 \\ J_1 & J_2 \end{bmatrix},$$

where

$$F = \begin{pmatrix} \frac{k^2\alpha_1\varepsilon_1 P(k,k^\Delta)}{(\delta_1+\varepsilon_1)\langle k\rangle} & \frac{k^2\alpha_1\varepsilon_1 P(k,k^\Delta)}{(\delta_1+\varepsilon_1)\langle k\rangle} \\ \frac{k^2\lambda_1\delta_1 P(k,k^\Delta)}{(\delta_1+\varepsilon_1)\langle k\rangle} & \frac{k^2\lambda_1\delta_1 P(k,k^\Delta)}{(\delta_1+\varepsilon_1)\langle k\rangle} \end{pmatrix},$$

$$V = \begin{pmatrix} \delta_1+\gamma_1 & -\varepsilon_1 \\ -\delta_1 & \varepsilon_1+\eta_1 \end{pmatrix}.$$

Thus (28), as shown at the bottom of the page. Then we can obtain the spectral radius of FV^{-1}

$$R_0 = \frac{k^2 P(k,k^\Delta)[\alpha_1\varepsilon_1(\delta_1+\varepsilon_1+\eta_1)+\lambda_1\delta_1(\delta_1+\varepsilon_1+\gamma_1)]}{\langle k\rangle(\varepsilon_1+\delta_1)[(\delta_1+\gamma_1)(\varepsilon_1+\eta_1)-\varepsilon_1\delta_1]} \tag{29}$$

It can be seen that the basic reproduction number is closely related to the initial impact and the spatiotemporal evolution of public health emergency. These factors have an important effect on the information spreading under public health emergency. In particular, as the probability α_1, λ_1 reflect the initial impact of the public health emergency, when the value of α_1, λ_1 make the basic reproduction number greater than 1, the public health emergency information will gradually spread.

IV. NUMERICAL SIMULATIONS

In this section, we perform numerical simulations to validate the effectiveness of model. As the similar results between numerical simulations and real data experiments, we analyze the dynamics of the model through numerical simulations in further. Besides, when there are more stages in the evolution of public health emergency, we can roughly divide the two adjacent stages into a group for analysis in turn. For simplicity, we take two stages as an example for simulation analysis.

A. MODEL VERIFICATION

The outbreak of COVID-19 suddenly made individuals become highly panicked and anxious. In particular, because the novel coronavirus is a new virus, individuals know little about it. This led to infection symptoms becoming the focus that individuals concerned. Therefore, we take the novel coronavirus infection symptoms as an example to analyze the effectiveness of the model $S_1S_2I_1I_2R$. Based on massive Baidu user behavior data, Baidu Index makes a statistical analysis of the change of the Chinese people's attention to a certain keyword, so it is widely used by scholars to study the changing trend of information [59]. As shown in Fig. 3(a), with the term "What are the symptoms of the novel coronavirus", we use Baidu Index to show the spreading trend of relevant information from January 20, 2020 to February 20, 2020.[1]

In the simulation of $S_1S_2I_1I_2R$ model, we take a connected subnet in the social network as an example, and assume that there are 1000 individuals in the network. As the patients detected at that time were mainly concentrated in a few areas, it is assumed that there are 100 individuals in affected areas and 900 individuals in not affected areas. Considering the power law distribution of the node degree in social network, we choose the typical Barabasi Albert (BA)

[1] https://index.baidu.com/v2/index.html

$$F(x) = \begin{bmatrix} k\alpha_1\rho^{S_1}(k,k^\Delta,t)w + k^\Delta\alpha_1^\Delta\rho^{S_1}(k,k^\Delta,t)\varphi \\ k\lambda_1\rho^{S_2}(k,k^\Delta,t)w + k^\Delta\lambda_1^\Delta\rho^{S_2}(k,k^\Delta,t)\varphi \\ 0 \\ 0 \\ 0 \end{bmatrix} \tag{26}$$

$$V(x) = \begin{bmatrix} \delta_1\rho^{I_1}(k,k^\Delta,t) - \varepsilon_1\rho^{I_2}(k,k^\Delta,t) + \gamma_1\rho^{I_1}(k,k^\Delta,t) \\ \varepsilon_1\rho^{I_2}(k,k^\Delta,t) - \delta_1\rho^{I_1}(k,k^\Delta,t) + \eta_1\rho^{I_2}(k,k^\Delta,t) \\ -(k\beta_1 w + k^\Delta\beta_1^\Delta\varphi)\rho^{S_1}(k,k^\Delta,t) - (k\xi_1 w + k^\Delta\xi_1^\Delta\varphi)\rho^{S_2}(k,k^\Delta,t) - \gamma_1\rho^{I_1}(k,k^\Delta,t) - \eta_1\rho^{I_2}(k,k^\Delta,t) \\ k(\alpha_1+\beta_1)\rho^{S_1}(k,k^\Delta,t)w + k^\Delta(\alpha_1^\Delta+\beta_1^\Delta)\rho^{S_1}(k,k^\Delta,t)\varphi + \delta_1\rho^{S_1}(k,k^\Delta,t) - \varepsilon_1\rho^{S_2}(k,k^\Delta,t) \\ k(\lambda_1+\xi_1)\rho^{S_2}(k,k^\Delta,t)w + k^\Delta(\lambda_1^\Delta+\xi_1^\Delta)\rho^{S_2}(k,k^\Delta,t)\varphi + \varepsilon_1\rho^{S_2}(k,k^\Delta,t) - \delta_1\rho^{S_1}(k,k^\Delta,t) \end{bmatrix} \tag{27}$$

$$FV^{-1} = \begin{bmatrix} \frac{k^2P(k,k^\Delta)\alpha_1\varepsilon_1(\delta_1+\varepsilon_1+\eta_1)}{\langle k\rangle(\varepsilon_1+\delta_1)[(\delta_1+\gamma_1)(\varepsilon_1+\eta_1)-\varepsilon_1\delta_1]} & \frac{k^2P(k,k^\Delta)\alpha_1\varepsilon_1(\delta_1+\varepsilon_1+\gamma_1)}{\langle k\rangle(\varepsilon_1+\delta_1)[(\delta_1+\gamma_1)(\varepsilon_1+\eta_1)-\varepsilon_1\delta_1]} \\ \frac{k^2P(k,k^\Delta)\lambda_1\delta_1(\delta_1+\varepsilon_1+\eta_1)}{\langle k\rangle(\varepsilon_1+\delta_1)[(\delta_1+\gamma_1)(\varepsilon_1+\eta_1)-\varepsilon_1\delta_1]} & \frac{k^2P(k,k^\Delta)\lambda_1\delta_1(\delta_1+\varepsilon_1+\gamma_1)}{\langle k\rangle(\varepsilon_1+\delta_1)[(\delta_1+\gamma_1)(\varepsilon_1+\eta_1)-\varepsilon_1\delta_1]} \end{bmatrix} \tag{28}$$

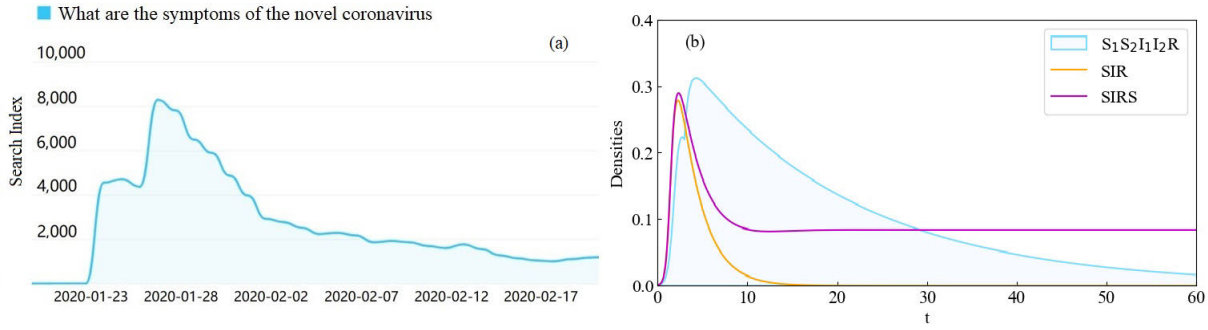

FIGURE 3. Comparison between public health emergency information about "What are the symptoms of the novel coronavirus" and model simulation results. (a) Baidu Index of the term "What are the symptoms of the novel coronavirus". (b) Simulation results of $S_1S_2I_1I_2R$, SIR and SIRS models. The blue area shows the result of $S_1S_2I_1I_2R$ model, the red line shows the result of SIR model, and the purple line shows the result of SIRS model.

scale-free network to construct the spreading networks in affected areas and not affected areas. According to Ref. [49], we set the average degree of nodes in each network is 12, and the amount of 2-simplices within which each node may locate is 4. To connect the affected network and not affected network, five nodes are randomly selected from the two networks to connect with each other. In addition, considering that the individuals in affected areas could obtain and spread the relevant information earlier, we assume the density of spreaders in affected areas is 0.001, and the density of susceptibles in affected areas is 0.099, and others are all susceptibles in not affected areas. As the number of patients were gradually increasing, and Academician Zhong Nanshan said that the virus could spread from human to human on January 20, 2020 [60], individuals in affected areas were eager to know the symptoms of novel coronavirus, and spread relevant information with strong willingness. Thus, we assume that $\alpha_1 = 0.4$, $\beta_1 = 0.3$, $\gamma_1 = 0.35$. While for the individuals in not affected areas, because cases had not been reported and it was the Lunar New Year, the willingness to spread relevant information was slightly weaker. Thus, we assume that $\lambda_1 = 0.2$, $\xi_1 = 0.4$, $\eta_1 = 0.5$. Moreover, facing with the public health emergency, the 2-simplex interactions would promote the information spreading significantly. Thus, we set $\mu = 1.2$, $\sigma = 0.8$, then $\alpha_1^{\Delta} = 0.48$, $\beta_1^{\Delta} = 0.24$, $\lambda_1^{\Delta} = 0.24$, $\xi_1^{\Delta} = 0.32$. Besides, as the Spring Festival travel in China had begun at that time, there was a large passenger flowing. This resulted that the virus gradually spread to other areas. Especially, COVID-19 has an incubation period, and individuals' protection awareness were not strong. This resulted that more and more areas turned into the affected areas. Thus, it is assumed that $\delta_1 = 0.1$, $\varepsilon_1 = 0.12$. In addition, due to the increasingly severe epidemic situation from late January 2020 to early February 2020, individuals were more frightened and more inclined to spread the information, the evolution of the public health emergency in this period could be divided into two stages, and the second stage was gradually deteriorating. Thus, we set $\theta_2 = 2$, $\delta_2 = 0.07$, $\varepsilon_2 = 0.15$, and $t_2 = 3$.

The simulation result of $S_1S_2I_1I_2R$ model is shown in the blue area of Fig. 3(b). Furthermore, we compare the result with simulation results of SIR and SIRS models. Here, the network structure remains unchanged. Considering that the regional difference is not taken into account in these models, the density of spreaders is set as 0.001, the density of susceptibles is set as 0.999, and the densities of others are set as 0 at the initial moment. For simplicity, we set the transition probability that a susceptible turns into a spreader in the model SIR and SIRS are all 0.3 through simple arithmetic average. By the same way, the transition probability that a susceptible turns into a recovered is set as 0.35 and the transition probability that a spreader turns into a recovered is set as 0.425 in SIR and SIRS models. Moreover, we set the transition probabilities that a recovered turns into a susceptible is 0.1 in model SIRS. These simulation results are shown with red and purple lines. Compared Fig. 3(a) with Fig. 3(b), we can find that the simulation result of the $S_1S_2I_1I_2R$ model is consistent with the spreading trend of information about ''What are the symptoms of the novel coronavirus''. However, the traditional SIR model and the improved model SIRS are difficult to describe the multi-stage information spreading process under public health emergency effectively for the reason that they do not consider the effect of emergency evolution, regional differences, and 2-simplex interactions. Thus, the $S_1S_2I_1I_2R$ model is more effective.

B. MULTI-STAGE INFORMATION SPREADING UNDER PUBLIC HEALTH EMERGENCY

In order to further analyze the changing trend of individuals in each state, we perform the numerical simulation by setting the same value of each parameter and the proportion of initial states as in Subsection MODEL VERIFICATION. As shown in Fig. 4, compared with the previous single-stage information spreading, the densities' variation trends present different characteristics. On the one hand, there are significant differences between affected areas and not affected areas. For example, the density of individuals in state S_2 decreases continuously until the system reaches a stable state, while the density of individuals in state S_1 increases firstly

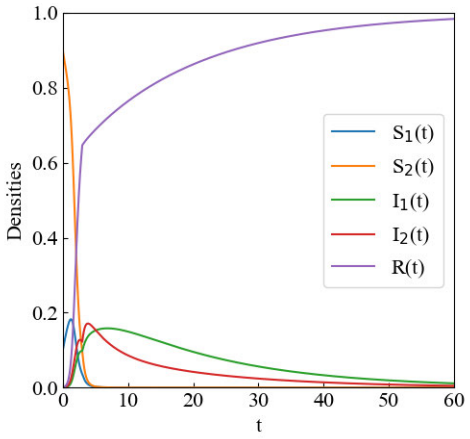

FIGURE 4. Information spreading process under public health emergency. We set $\alpha_1 = 0.4$, $\alpha_1^{\Delta} = 0.48$, $\beta_1 = 0.3$, $\beta_1^{\Delta} = 0.24$, $\gamma_1 = 0.35$, $\lambda_1 = 0.2$, $\lambda_1^{\Delta} = 0.24$, $\xi_1 = 0.4$, $\xi_1^{\Delta} = 0.32$, $\eta_1 = 0.5$, $\delta_1 = 0.1$, $\varepsilon_1 = 0.12$, $\theta_2 = 2$, $\delta_2 = 0.07$, $\varepsilon_2 = 0.15$, and $t_2 = 3$.

and then decreases. On the other hand, the density curves of individuals in state I_1 and I_2 have two stages and the density curve of individuals in state I_2 changes faster and the peak value is larger than that in state I_1 as the initial number of individuals in not affected areas is larger. In particular, the density curves of individuals in state I_1 and I_2 have two peaks, and both of them present a trend of rising and falling, and then rising and falling again. Especially, the decrease rate of the density curve of individuals in state I_1 is slower as more and more not affected areas becoming affected areas. In addition, although the variation trend of individuals in state R is rising as previous research results, the growth rate of the curve slows down significantly at the second stage. The main reason for these trends is that at the initial moment, only a few of the individuals in affected areas know little about it, and most of individuals might think it is a common disease, so they are not willing to spread the information and have a weak protection awareness. However, with the movement of individuals and the spread of the virus, the coverage areas become more and more extensive, the public health emergency gradually gets worse. This results that the individuals become more and more panic and spread the information for a long time. Especially, the number of spreaders may even rebound. Thus, the growth rate of recovereds becomes slow gradually.

In fact, the variation trends presented in Fig. 4 are consistent with the real situation. Take the information spreading process of symptoms of COVID-19 as an example. On January 20, 2020, Academician Zhong Nanshan said that the virus could spread from human to human [60]. Besides, National Health Commission of the People's Republic of China published the situation of COVID-19 every day since then. This resulted that more and more individuals were eager to obtain and spread relevant information. As the number of infected people gradually increased and confirmed cases were reported in many regions, the public health emergency became severe increasingly and individuals became more panic. This led to the further spread of public health emergency information and the second stage of spreading.

C. EFFECT OF 2-SIMPLEX INTERACTIONS

Except for the basis of pairwise interactions, high-order interactions among individuals also affect the information spreading. Here we perform numerical simulations to analyze the effect of 2-simplex interactions on the information spreading. The spreading network and initial state ratios are the same as those in Subsection MODEL VERIFICATION. The cross-regional spatial evolution is not taken into account, and $\delta_1 = \delta_2 = \varepsilon_1 = \varepsilon_2$. Besides, the local evolution of public health emergency in affected areas is also not considered here, i.e., $\theta_1 = \theta_2 = 0$. Considering the maximum sum of the densities of the two categories of spreaders reflects the information's maximum impact, and the maximum density of the recovereds reflects the final spreading scale of the information, we mainly pay attention to the changes of these two densities.

The effect of 2-simplex interactions on individuals mainly lies in two aspects. On the one hand, it would affect the transition from susceptibles to spreaders. On the other hand, it would affect the transition from susceptibles to recovereds. Therefore, as shown in Fig. 5, we describe the changes densities of the two categories of spreaders and recovereds with μ to reveal the effect of 2-simplex interactions on susceptibles turning into corresponding spreaders. Similarly, as shown in Fig. 6, we describe the changes densities of the two categories of spreaders and recovereds with σ to reveal the effect of 2-simplex interactions on susceptibles turning into recovereds. Here, when $\mu = 0$, and $\sigma = 0$, there is no 2-simplex interactions. We can see that comparing with the single pairwise interactions, the process of information spreading under the effect of 2-simplex interactions shows the significant difference. Specially, with the increase of μ, both the information's maximum impact and the spreading scale increase. While on the contrary, with the increase of σ, both the information's maximum impact and the spreading scale decrease. That is to say, the 2-simplex interactions have significant effect on the information spreading. The greater the effect of 2-simplex interactions on the transformation from susceptibles to corresponding spreaders, and the weaker the effect of 2-simplex interactions on the transformation from susceptibles to recovereds, the faster and wider information spreading.

D. EFFECT OF THE PUBLIC HEALTH EMERGENCY'S INITIAL IMPACT

As we all know, α_1, α_1^{Δ}, λ_1, λ_1^{Δ} are important parameters to describe the initial impact of the public health emergency. Here we perform numerical simulations to analyze the effect of public health emergency's initial impact on the information spreading under four different situations, respectively. The spreading network and initial state ratios are the same as those in Subsection MODEL VERIFICATION. Besides,

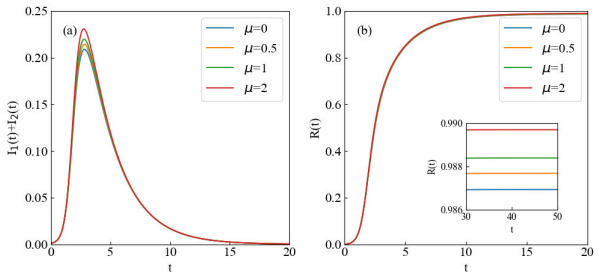

FIGURE 5. Effect of 2-simplex interactions on susceptibles turning into spreaders. (a) The density of two categories of spreaders with the increase of μ. (b) The density of recovereds with the increase of μ. We set $\sigma = 0$, $\alpha_1 = 0.4$, $\beta_1 = 0.3$, $\gamma_1 = 0.35$, $\lambda_1 = 0.2$, $\xi_1 = 0.4$, $\eta_1 = 0.5$, $\delta_1 = 0.1$, $\varepsilon_1 = 0.1$, $\theta_2 = 0$, $\delta_2 = 0.1$, $\varepsilon_2 = 0.1$, and $t_2 = 3$.

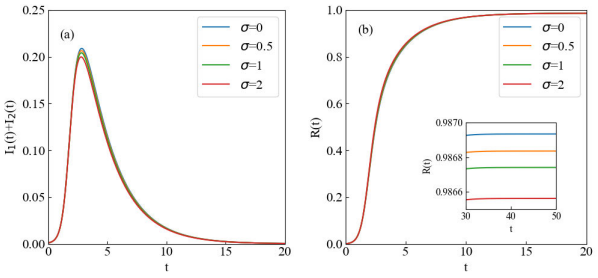

FIGURE 6. Effect of 2-simplex interactions on susceptibles turning into recovereds. (a) The density of two categories of spreaders with the increase of σ. (b) The density of recovereds with the increase of σ. We set $\mu = 0$, $\alpha_1 = 0.4$, $\beta_1 = 0.3$, $\gamma_1 = 0.35$, $\lambda_1 = 0.2$, $\xi_1 = 0.4$, $\eta_1 = 0.5$, $\delta_1 = 0.1$, $\varepsilon_1 = 0.1$, $\theta_2 = 0$, $\delta_2 = 0.1$, $\varepsilon_2 = 0.1$, and $t_2 = 3$.

considering the 2-simplex interactions usually stimulate the propagation willingness and promote the information spreading, we set $\mu = 1.2$, $\sigma = 0.8$.

1) EFFECT OF THE INITIAL IMPACT WITH LOCAL EVOLUTION OF PUBLIC HEALTH EMERGENCY

The local evolution of public health emergency includes deterioration and improvement in affected areas. The cross-regional spatial evolution is not taken into account, and $\delta_1 = \delta_2 = \varepsilon_1 = \varepsilon_2$. As shown in Fig. 7-Fig. 10, we describe the changes densities of the two categories of spreaders and recovereds with α_1, α_1^Δ, λ_1, λ_1^Δ to reveal the effect of the public health emergency's initial impact on the information spreading under two local evolution situations.

According to the numerical simulations results in Fig. 7-Fig. 10, it can be seen that the information is widely spread. Observing Fig. 7-Fig. 10, we can find that at the first stage, the change rates of the two categories of spreaders and recovereds gradually speed up with the increase of $\alpha_1, \alpha_1^\Delta, \lambda_1, \lambda_1^\Delta$. Besides, the peak value of the two categories of spreaders and the information spreading scale also gradually increase. However, compared the curves' trends at the second stage in Fig. 7-Fig. 8 with Fig. 9-Fig. 10, we can find that the decrease rates of the densities of the two categories of spreaders slow down significantly, and even rebound to produce new peaks when the public health emergency gradually worsens

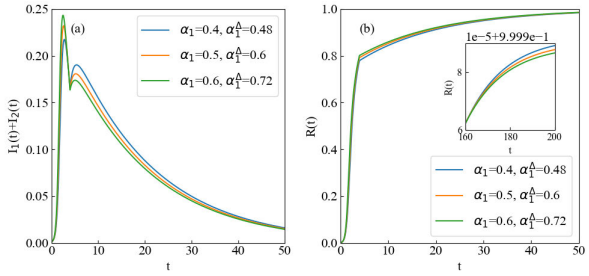

FIGURE 7. Effect of public health emergency's initial impact in affected areas on information spreading under local deterioration. (a) The density of two categories of spreaders with the increase of α_1, α_1^Δ. (b) The density of recovereds with the increase of α_1, α_1^Δ. We set $\beta_1 = 0.3$, $\beta_1^\Delta = 0.24$, $\gamma_1 = 0.35$, $\lambda_1 = 0.2$, $\lambda_1^\Delta = 0.24$, $\xi_1 = 0.4$, $\xi_1^\Delta = 0.32$, $\eta_1 = 0.5$, $\theta_1 = 0$, $\theta_2 = 2$, $\delta_1 = \delta_2 = \varepsilon_1 = \varepsilon_2 = 0.1$, $t_2 = 4$, respectively. The transition probabilities at the second stage could be determined according to Equation (1) and Equation (2), respectively. The blue lines denote the densities of two categories of spreaders and recovereds in each time with $\alpha_1 = 0.4$, $\alpha_1^\Delta = 0.48$. The orange lines denote the densities of two categories of spreaders and recovereds in each time with $\alpha_1 = 0.5$, $\alpha_1^\Delta = 0.6$. The green lines denote the densities of two categories of spreaders and recovereds in each time with $\alpha_1 = 0.6$, $\alpha_1^\Delta = 0.72$.

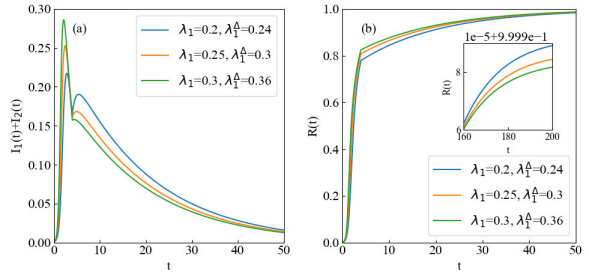

FIGURE 8. Effect of public health emergency's initial impact in not affected areas on information spreading under local deterioration. (a) The density of two categories of spreaders with the increase of λ_1, λ_1^Δ. (b) The density of recovereds with the increase of λ_1, λ_1^Δ. We set $\alpha_1 = 0.4$, $\alpha_1^\Delta = 0.48$, $\beta_1 = 0.3$, $\beta_1^\Delta = 0.24$, $\gamma_1 = 0.35$, $\xi_1 = 0.4$, $\xi_1^\Delta = 0.32$, $\eta_1 = 0.5$, $\theta_1 = 0$, $\theta_2 = 2$, $\delta_1 = \delta_2 = \varepsilon_1 = \varepsilon_2 = 0.1$, $t_2 = 4$, respectively. The transition probabilities at the second stage could be determined according to Equation (1) and Equation (2), respectively. The blue lines denote the densities of two categories of spreaders and recovereds in each time with $\lambda_1 = 0.2$, $\lambda_1^\Delta = 0.24$. The orange lines denote the densities of two categories of spreaders and recovereds in each time with $\lambda_1 = 0.25$, $\lambda_1^\Delta = 0.3$. The green lines denote the densities of two categories of spreaders and recovereds in each time with $\lambda_1 = 0.3$, $\lambda_1^\Delta = 0.36$.

in affected areas. Moreover, the growth rates of recovereds also slow down significantly compared with the first stage. However, when the public health emergency in affected areas gradually getting improved, the decrease rates of the two categories of spreaders and the growth rates of recovereds increase rapidly at the second stage. In addition, according to the densities' changes of the two categories of spreaders and recovereds at two stages in Fig. 7-Fig. 8, it can be found that the maximum densities and change speeds of the two categories of spreaders and recovereds are larger when α_1, α_1^Δ, λ_1, λ_1^Δ are relatively low. This is different from the trend at the first stage. It could be explained as follows. On the one hand, the low initial attraction at the first stage might not arouse individuals' attention, and most of

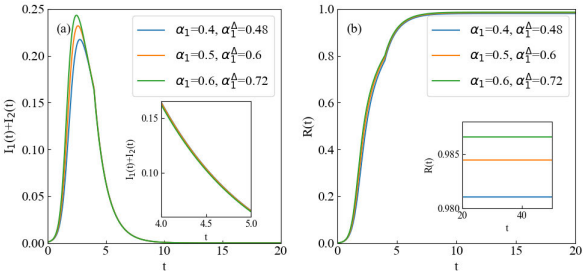

FIGURE 9. Effect of public health emergency's initial impact in affected areas on information spreading under local improvement. (a) The density of two categories of spreaders with the increase of α_1, α_1^Δ. (b) The density of recovereds with the increase of α_1, α_1^Δ. We set $\beta_1 = 0.3$, $\beta_1^\Delta = 0.24$, $\gamma_1 = 0.35$, $\lambda_1 = 0.2$, $\lambda_1^\Delta = 0.24$, $\xi_1 = 0.4$, $\xi_1^\Delta = 0.32$, $\eta_1 = 0.5$, $\theta_1 = 0$, $\theta_2 = 2$, $\delta_1 = \delta_2 = \varepsilon_1 = \varepsilon_2 = 0.1$, $t_2 = 4$, respectively. The transition probabilities at the second stage could be determined according to Equation (1) and Equation (2), respectively. The blue lines denote the densities of two categories of spreaders and recovereds in each time with $\alpha_1 = 0.4$, $\alpha_1^\Delta = 0.48$. The orange lines denote the densities of two categories of spreaders and recovereds in each time with $\alpha_1 = 0.5$, $\alpha_1^\Delta = 0.6$. The green lines denote the densities of two categories of spreaders and recovereds in each time with $\alpha_1 = 0.6$, $\alpha_1^\Delta = 0.72$.

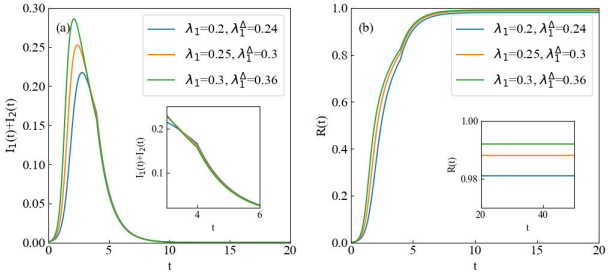

FIGURE 10. Effect of public health emergency's initial impact in not affected areas on information spreading under local improvement. (a) The density of two categories of spreaders with the increase of λ_1, λ_1^Δ. (b) The density of recovereds with the increase of λ_1, λ_1^Δ. We set $\alpha_1 = 0.4$, $\alpha_1^\Delta = 0.48$, $\beta_1 = 0.3$, $\beta_1^\Delta = 0.24$, $\gamma_1 = 0.35$, $\xi_1 = 0.4$, $\xi_1^\Delta = 0.32$, $\eta_1 = 0.5$, $\theta_1 = 0$, $\theta_2 = 2$, $\delta_1 = \delta_2 = \varepsilon_1 = \varepsilon_2 = 0.1$, $t_2 = 4$, respectively. The transition probabilities at the second stage could be determined according to Equation (1) and Equation (2), respectively. The blue lines denote the densities of two categories of spreaders and recovereds in each time with $\lambda_1 = 0.2$, $\lambda_1^\Delta = 0.24$. The orange lines denote the densities of two categories of spreaders and recovereds in each time with $\lambda_1 = 0.25$, $\lambda_1^\Delta = 0.3$. The green lines denote the densities of two categories of spreaders and recovereds in each time with $\lambda_1 = 0.3$, $\lambda_1^\Delta = 0.36$.

them are susceptibles. As a result, much more susceptibles become anxious and spread information quickly when public health emergency deteriorating. On the other hand, the decline rate of the two categories of spreaders is slow at the first stage when the initial impact is small. This leads to more individuals in states I_1 and I_2 when the public health emergency deteriorating. Specially, the probabilities of two categories of spreaders turning into recovereds decrease at the second stage. This results in a larger maximum density of the two categories of spreaders and recovereds.

According to the above analysis, the initial impact and local evolution trend of public health emergency have an important effect on individuals' behaviors. This result inspires the government to take strong prevention and control measures to promote emergency improvement, and stabilize individuals' sentiment in further. Especially, the government should not relax the guidance when the individuals' willingness to spread the information at the early stage is not strong. It is helpful to weaken the negative impact of misinformation.

2) EFFECT OF THE INITIAL IMPACT WITH SPATIAL EVOLUTION OF PUBLIC HEALTH EMERGENCY

The spatial evolution of public health emergency is mainly reflected by the probability of interaction between affected areas and not affected areas. The local evolution of public health emergency in affected areas is not considered here, i.e., $\theta_1 = \theta_2 = 0$. If the probability that individuals transmit from affected areas to not affected areas decreases, while the probability that individuals transmit from not affected areas to affected areas increases, it indicates that the public health emergency deteriorates in space. On the contrary, if the probability that individuals transmit from affected areas to not affected areas increases, while the probability that individuals transmit from not affected areas to affected areas decreases, it indicates that the public health emergency is getting improved in space. Thus, as the numerical simulations results shown in Fig. 11-Fig. 14, the density changes of the two categories of spreaders and recovereds with α_1, α_1^Δ, λ_1, λ_1^Δ under the two situations are mainly analyzed, so as to reveal the effect of initial impact on the information spreading under the spatial evolution of public health emergency.

Observing Fig. 11-Fig. 14, we can find that with the increase of α_1, α_1^Δ, λ_1, λ_1^Δ, both the change speeds of the densities of the two categories of spreaders and recovereds gradually speed up, and the peak value of the two categories of spreaders and the information spreading scale also gradually increase no matter the public health emergency worsens or gets better in space. Meanwhile, compared Fig. 11 and Fig. 13 with Fig. 12 and Fig. 14, we can also find that the changes are much larger when the initial impact of public health emergency on not affected areas increases. The above results indicate that the initial impact plays an important role in the information spreading regardless of deterioration or improvement in space.

E. EFFECT OF THE LOCAL EVOLUTION OF PUBLIC HEALTH EMERGENCY

According to the above analysis, the dynamic evolution of public health emergency has an important effect on the information spreading. Here, the effects of deterioration and improvement of public health emergency in affected areas are analyzed firstly, and the impact of cross-regional spatial evolution is ignored now. Therefore, it is assumed that the transition probabilities of individuals between affected areas and not affected areas are the same and unchanged, i.e., $\delta_1 = \delta_2 = \varepsilon_1 = \varepsilon_2$. Similar to the above, we also set $\mu = 1.2$, $\sigma = 0.8$. The effects of local evolution degree and time of public health emergency on the information spreading are analyzed through numerical simulations, respectively. Based on the

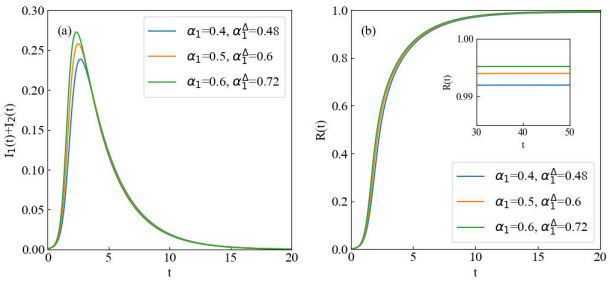

FIGURE 11. Effect of public health emergency's initial impact in affected areas on information spreading under spatial deterioration. (a) The density of two categories of spreaders with the increase of α_1, α_1^Δ. (b) The density of recovereds with the increase of α_1, α_1^Δ. We set $\beta_1 = 0.3$, $\beta_1^\Delta = 0.24$, $\gamma_1 = 0.35$, $\lambda_1 = 0.2$, $\lambda_1^\Delta = 0.24$, $\xi_1 = 0.4$, $\xi_1^\Delta = 0.32$, $\eta_1 = 0.5$, $\theta_1 = \theta_2 = 0$, $\delta_1 = \varepsilon_1 = 0.2$, $\delta_2 = 0.1$, $\varepsilon_2 = 0.3$. The blue lines denote the densities of two categories of spreaders and recovereds in each time with $\alpha_1 = 0.4$, $\alpha_1^\Delta = 0.48$. The orange lines denote the densities of two categories of spreaders and recovereds in each time with $\alpha_1 = 0.5$, $\alpha_1^\Delta = 0.6$. The green lines denote the densities of two categories of spreaders and recovereds in each time with $\alpha_1 = 0.6$, $\alpha_1^\Delta = 0.72$.

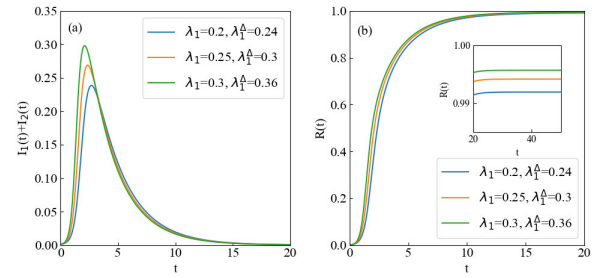

FIGURE 12. Effect of public health emergency's initial impact in not affected areas on information spreading under spatial deterioration. (a) The density of two categories of spreaders with the increase of λ_1, λ_1^Δ. (b) The density of recovereds with the increase of λ_1, λ_1^Δ. We set $\alpha_1 = 0.4$, $\alpha_1^\Delta = 0.48$, $\beta_1 = 0.3$, $\beta_1^\Delta = 0.24$, $\gamma_1 = 0.35$, $\xi_1 = 0.4$, $\xi_1^\Delta = 0.32$, $\eta_1 = 0.5$, $\theta_1 = \theta_2 = 0$, $\delta_1 = \varepsilon_1 = 0.2$, $\delta_2 = 0.1$, $\varepsilon_2 = 0.3$. The blue lines denote the densities of two categories of spreaders and recovereds in each time with $\lambda_1 = 0.2$, $\lambda_1^\Delta = 0.24$. The orange lines denote the densities of two categories of spreaders and recovereds in each time with $\lambda_1 = 0.25$, $\lambda_1^\Delta = 0.3$. The green lines denote the densities of two categories of spreaders and recovereds in each time with $\lambda_1 = 0.3$, $\lambda_1^\Delta = 0.36$.

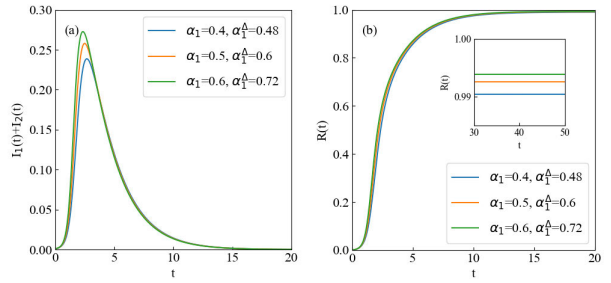

FIGURE 13. Effect of public health emergency's initial impact in affected areas on information spreading under spatial improvement. (a) The density of two categories of spreaders with the increase of α_1, α_1^Δ. (b) The density of recovereds with the increase of α_1, α_1^Δ. We set $\beta_1 = 0.3$, $\beta_1^\Delta = 0.24$, $\gamma_1 = 0.35$, $\lambda_1 = 0.2$, $\lambda_1^\Delta = 0.24$, $\xi_1 = 0.4$, $\xi_1^\Delta = 0.32$, $\eta_1 = 0.5$, $\theta_1 = \theta_2 = 0$, $\delta_1 = \varepsilon_1 = 0.2$, $\delta_2 = 0.3$, $\varepsilon_2 = 0.1$. The blue lines denote the densities of two categories of spreaders and recovereds in each time with $\alpha_1 = 0.4$, $\alpha_1^\Delta = 0.48$. The orange lines denote the densities of two categories of spreaders and recovereds in each time with $\alpha_1 = 0.5$, $\alpha_1^\Delta = 0.6$. The green lines denote the densities of two categories of spreaders and recovereds in each time with $\alpha_1 = 0.6$, $\alpha_1^\Delta = 0.72$.

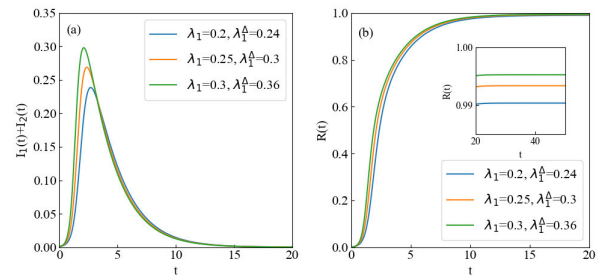

FIGURE 14. Effect of public health emergency's initial impact in not affected areas on information spreading under spatial improvement. (a) The density of two categories of spreaders with the increase of λ_1, λ_1^Δ. (b) The density of recovereds with the increase of λ_1, λ_1^Δ. We set $\alpha_1 = 0.4$, $\alpha_1^\Delta = 0.48$, $\beta_1 = 0.3$, $\beta_1^\Delta = 0.24$, $\gamma_1 = 0.35$, $\xi_1 = 0.4$, $\xi_1^\Delta = 0.32$, $\eta_1 = 0.5$, $\theta_1 = \theta_2 = 0$, $\delta_1 = \varepsilon_1 = 0.2$, $\delta_2 = 0.3$, $\varepsilon_2 = 0.1$. The blue lines denote the densities of two categories of spreaders and recovereds in each time with $\lambda_1 = 0.2$, $\lambda_1^\Delta = 0.24$. The orange lines denote the densities of two categories of spreaders and recovereds in each time with $\lambda_1 = 0.25$, $\lambda_1^\Delta = 0.3$. The green lines denote the densities of two categories of spreaders and recovereds in each time with $\lambda_1 = 0.3$, $\lambda_1^\Delta = 0.36$.

network construct in Subsection MODEL VERIFICATION and taking the same initial states setting, we study the effect of local evolution of public health emergency on the information spreading by analyzing the densities' changes of the two categories of spreaders and recovereds.

1) EFFECT OF THE LOCAL EVOLUTION DEGREE OF PUBLIC HEALTH EMERGENCY

The deterioration and improvement of public health emergency in affected areas have an important effect on individuals' behaviors. Here, the degree of local evolution of public health emergency can be reflected through θ_2. According to Subsection EFFECT OF EVOLUTION OF PUBLIC HEARLTH EMERGENCY ON STATES TRANSITION, the same evolution degree has different effects on individuals' behaviors when public health emergency worsening or improving, which can be reflected by calculating corresponding transition probabilities according to Equation (1) and Equation (2). As shown in Fig. 15 and Fig. 16, the densities' changes of the two categories of spreaders and recovereds along with the evolution degree under the two situations are described respectively.

From the numerical simulation result in Fig. 15(a), we can see that at the second stage, the peak value of the density curve of the two categories of spreaders increases gradually with the increase of θ_2, and the larger θ_2 is, the faster the increase rate before reaching the peak of the second stage, and the slower the decrease rate after reaching the peak of the second stage. In particular, the deterioration of public health emergency also makes the density of the two categories of spreaders rebound to produce a new peak at the second stage. In addition, it can be seen from the numerical simulation

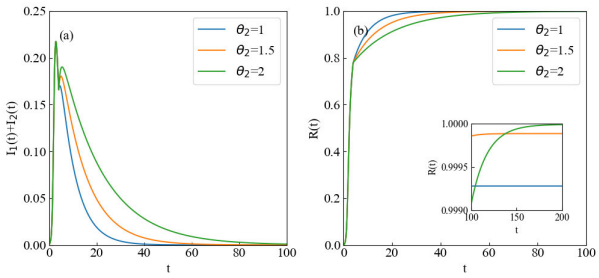

FIGURE 15. Effect of local deterioration degree of public health emergency on information spreading. (a) The density of two categories of spreaders with the increase of θ_2. (b) The density of recovereds with the increase of θ_2. We set $\alpha_1 = 0.4$, $\alpha_1^{\Delta} = 0.48$, $\beta_1 = 0.3$, $\beta_1^{\Delta} = 0.24$, $\gamma_1 = 0.35$, $\lambda_1 = 0.2$, $\lambda_1^{\Delta} = 0.24$, $\xi_1 = 0.4$, $\xi_1^{\Delta} = 0.32$, $\eta_1 = 0.5$, $\theta_1 = 0$, $\delta_1 = \delta_2 = \varepsilon_1 = \varepsilon_2 = 0.1$ and $t_2 = 4$, respectively. The blue lines denote the densities of two categories of spreaders and recovereds in each time with $\theta_2 = 1$. The orange lines denote the densities of two categories of spreaders and recovereds in each time with $\theta_2 = 1.5$. The green lines denote the densities of two categories of spreaders and recovereds in each time with $\theta_2 = 2$.

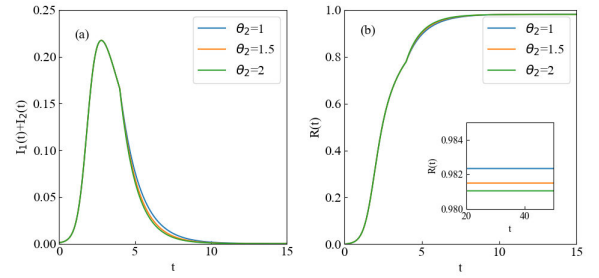

FIGURE 16. Effect of local improvement degree of public health emergency on information spreading. (a) The density of two categories of spreaders with the increase of θ_2. (b) The density of recovereds with the increase of θ_2. We set $\alpha_1 = 0.4$, $\alpha_1^{\Delta} = 0.48$, $\beta_1 = 0.3$, $\beta_1^{\Delta} = 0.24$, $\gamma_1 = 0.35$, $\lambda_1 = 0.2$, $\lambda_1^{\Delta} = 0.24$, $\xi_1 = 0.4$, $\xi_1^{\Delta} = 0.32$, $\eta_1 = 0.5$, $\theta_1 = 0$, $\delta_1 = \delta_2 = \varepsilon_1 = \varepsilon_2 = 0.1$ and $t_2 = 4$, respectively. The blue lines denote the densities of two categories of spreaders and recovereds in each time with $\theta_2 = 1$. The orange lines denote the densities of two categories of spreaders and recovereds in each time with $\theta_2 = 1.5$. The green lines denote the densities of two categories of spreaders and recovereds in each time with $\theta_2 = 2$.

result in Fig. 15(b) that at the second stage, the increase rate of recovereds' density gradually slows down with the increase of θ_2. This results that the recovereds' density under the high evolution degree is smaller than that under the low evolution degree in a period of time, but the maximum density of recovereds' density increases with the increase of θ_2. This is mainly because that the local deterioration of public health emergency in affected areas makes the susceptibles willing to spread the information much more, and makes the spreaders continue to spread for a long time. As a result, the information spreading cycle is extended, and the effect and the final spreading scale are also gradually expanded. By contrast, the numerical simulation result in Fig. 16 shows that with the local improvement of public health emergency at the second stage, the density of the two categories of spreaders decreases rapidly, and the greater the improvement degree, the faster the decrease rate of the density of the two categories of spreaders. This leads to much more individuals turn into recovereds, resulting in a faster increasing in the density of recovereds and declining in the spreading scale. These results indicate that the local evolution degree of public health emergency has an important effect on the information spreading. The greater the deterioration degree, the greater the effect and information spreading scale, while the greater the improvement degree, the more helpful to weaken the negative impact of public health emergency information.

2) EFFECT OF THE LOCAL EVOLUTION TIME OF PUBLIC HEALTH EMERGENCY

The time of local evolution of public health emergency reflects the severity of the local situation. Fig. 17 and Fig. 18 describe the densities' changes of the two categories of spreaders and recovereds with the evolution time under the local deterioration and improvement of public health emergency respectively.

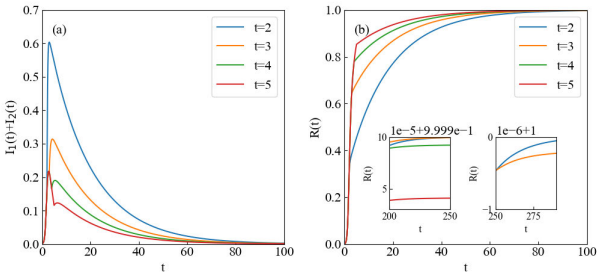

FIGURE 17. Effect of local deterioration time of public health emergency on information spreading. (a) The density of two categories of spreaders with the increase of t_2. (b) The density of recovereds with the increase of t_2. We set $\alpha_1 = 0.4$, $\alpha_1^{\Delta} = 0.48$, $\beta_1 = 0.3$, $\beta_1^{\Delta} = 0.24$, $\gamma_1 = 0.35$, $\lambda_1 = 0.2$, $\lambda_1^{\Delta} = 0.24$, $\xi_1 = 0.4$, $\xi_1^{\Delta} = 0.32$, $\eta_1 = 0.5$, $\theta_1 = 0$, $\theta_2 = 2$, $\delta_1 = \delta_2 = \varepsilon_1 = \varepsilon_2 = 0.1$, respectively. The blue lines denote the densities of two categories of spreaders and recovereds in each time with $t_2 = 2$. The orange lines denote the densities of two categories of spreaders and recovereds in each time with $t_2 = 3$. The green lines denote the densities of two categories of spreaders and recovereds in each time with $t_2 = 4$. The red lines denote the densities of two categories of spreaders and recovereds in each time with $t_2 = 5$.

As shown in Fig. 17, the earlier the local deterioration time of public health emergency, the larger the density peak of the two categories of spreaders and the maximum density of the recovereds. The numerical simulation result shows that the more rapid the deterioration of public health emergency and the more sudden the outbreak, the more individuals spread the information and the wider the information spreading scale. Besides, from the numerical simulation result in Fig. 17(a), we can find that if the local deterioration of public health emergency occurs before the arrival of the first peak, the density curve of the two categories of spreaders would become steeper rapidly. While if the local deterioration of public health emergency occurs just after the arrival of the first peak, the density curve of the two categories of spreaders would rebound quickly after a small decline and rise to produce a new peak. Besides, the earlier the local deterioration, the greater the peak value. This

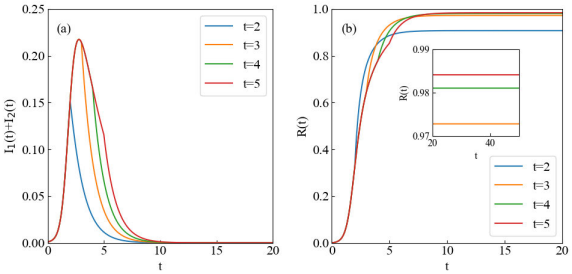

FIGURE 18. Effect of local improvement time of public health emergency on information spreading. (a) The density of two categories of spreaders with the increase of t_2. (b) The density of recovereds with the increase of t_2. We set $\alpha_1 = 0.4$, $\alpha_1^{\Delta} = 0.48$, $\beta_1 = 0.3$, $\beta_1^{\Delta} = 0.24$, $\gamma_1 = 0.35$, $\lambda_1 = 0.2$, $\lambda_1^{\Delta} = 0.24$, $\xi_1 = 0.4$, $\xi_1^{\Delta} = 0.32$, $\eta_1 = 0.5$, $\theta_1 = 0$, $\theta_2 = 2$, $\delta_1 = \delta_2 = \varepsilon_1 = \varepsilon_2 = 0.1$, respectively. The blue lines denote the densities of two categories of spreaders and recovereds in each time with $t_2 = 2$. The orange lines denote the densities of two categories of spreaders and recovereds in each time with $t_2 = 3$. The green lines denote the densities of two categories of spreaders and recovereds in each time with $t_2 = 4$. The red lines denote the densities of two categories of spreaders and recovereds in each time with $t_2 = 5$.

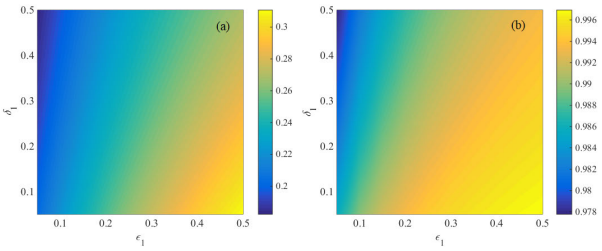

FIGURE 19. Effect of initial spatial transition probabilities on information spreading. We set $\alpha_1 = 0.4$, $\alpha_1^{\Delta} = 0.48$, $\beta_1 = 0.3$, $\beta_1^{\Delta} = 0.24$, $\gamma_1 = 0.35$, $\lambda_1 = 0.2$, $\lambda_1^{\Delta} = 0.24$, $\xi_1 = 0.4$, $\xi_1^{\Delta} = 0.32$, $\eta_1 = 0.5$, $t_2 = 3$. (a) The maximum sum of the densities of the two categories of spreaders as a function of δ_1 and ε_1. (b) The maximum density of the recovereds as a function of δ_1 and ε_1.

trend is mainly due to the fact that when the deterioration occurs at the beginning of information spreading, most of individuals are in state S_1 and S_2, and their panic would be intensified by the sudden deterioration of public health emergency. This makes their willingness to spread the public health emergency information be strengthened, and the number of spreaders increases rapidly. While if the deterioration occurs after the arrival of the first peak, on the one hand, the susceptibles would be stimulated to spread information, on the other hand, the spreaders would be promoted to continue spreading the information, thus the number of spreaders rebounds. However, because the majority of individuals have known the information and even become recovereds, the rebound peak of the density curve of two categories of spreaders would become smaller and the decline speed would be slower. On the contrary, from the numerical simulation result in Fig. 18, we can see that the earlier the local improvement, the more rapid the density of the two categories of spreaders decreases, and the smaller the maximum density of recovereds. In particular, it also can be seen from Fig. 18 that local improvement occurs before the density curve of the two categories of spreaders reaching the peak, the maximum impact of information would gradually decrease with the advance of the evolution time. These results suggest that the government should strengthen the monitoring of public health emergency and take timely measures to promote the improvement as soon as possible. It is important for controlling the spread of public health emergency information.

F. EFFECT OF THE SPATIAL EVOLUTION OF PUBLIC HEALTH EMERGENCY

In order to further study the effect of the spatial evolution of public health emergency, the effects of the interaction transition probabilities between affected areas and not affected areas on the information spreading are analyzed through numerical simulations, respectively. Here the effect of local evolution in affected areas is ignored, thus it is assumed that $\theta_1 = \theta_2 = 0$. As above, the spreading network and initial state ratios setting in Subsection MODEL VERIFICATION are used to study the effect of spatial evolution by analyzing the density changes of the two categories of spreaders and recovereds. Meanwhile, we also set $\mu = 1.2, \sigma = 0.8$.

1) EFFECT OF INITIAL SPATIAL TRANSITION PROBABILITIES

Fig. 19 depicts the changes of the maximum densities of two categories of spreaders and recovereds under the different initial spatial transition probabilities between affected areas and not affected areas. The effect of spatial evolution of public health emergency among different stages is not considered here, that is to say the corresponding probability of the same state transition at two stages is assumed to be the same.

As can be seen from Fig. 19, with the increase of the initial transition probability that affected areas turn into not affected areas, the maximum densities of two categories of spreaders and recovereds gradually decrease, while with the increase of the initial transition probability that not affected areas turn into affected areas, the maximum densities of two categories of spreaders and recovereds gradually increase. It indicates that the spatial evolution of public health emergency plays an important role in promoting the information spreading. Especially for a new public health emergency, individuals have little knowledge about it and lack of experience in effective prevention and control. It is easy to cause the cross regional diffusion of public health emergency, and trigger panic, so that more and more individuals pay attention to the relevant information. Especially at a special time like holidays, the human flow is often more frequent, thus the diffusion of the public health emergency would be more serious, and the information would also be more concerned. Besides, according to the diagonal color changes, we can find that the maximum sum of the densities of the two categories of spreaders and recovereds increase when δ_1 and ε_1 increasing synchronously. That means when the public health emergency in different regions getting worse or better

in succession, the information's maximum impact and the spreading scale would be enlarged.

2) EFFECT OF THE SPATIAL EVOLUTION DEGREE OF PUBLIC HEALTH EMERGENCY

Furthermore, we perform numerical simulations to analyze the effect of different spatial evolution degree at different stages on the information spreading. Here the density changes of the two categories of spreaders and the recovereds under different interaction transition probabilities between affected areas and not affected areas at the second stage are explored without considering the local deterioration and improvement. The numerical simulations results are shown in Fig. 20 and Fig. 21.

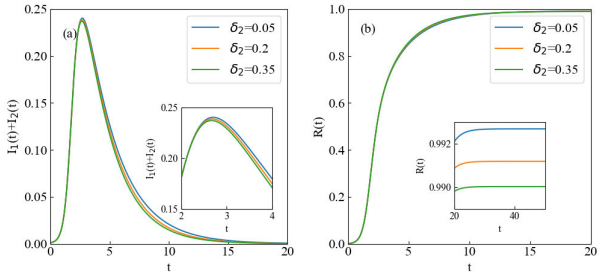

FIGURE 20. Effect of transition probability from affected area to not affected area at second stage on information spreading. (a) The density of two categories of spreaders with the increase of δ_2. (b) The density of recovereds with the increase of δ_2. We set $\alpha_1 = 0.4$, $\alpha_1^{\Delta} = 0.48$, $\beta_1 = 0.3$, $\beta_1^{\Delta} = 0.24$, $\gamma_1 = 0.35$, $\lambda_1 = 0.2$, $\lambda_1^{\Delta} = 0.24$, $\xi_1 = 0.4$, $\xi_1^{\Delta} = 0.32$, $\eta_1 = 0.5$, $\varepsilon_1 = \varepsilon_2 = 0.2$, $\delta_1 = 0.2$, $t_2 = 2$. The blue lines denote the densities of two categories of spreaders and recovereds in each time with $\delta_2 = 0.05$. The orange lines denote the densities of two categories of spreaders and recovereds in each time with $\delta_2 = 0.2$. The green lines denote the densities of two categories of spreaders and recovereds in each time with $\delta_2 = 0.35$.

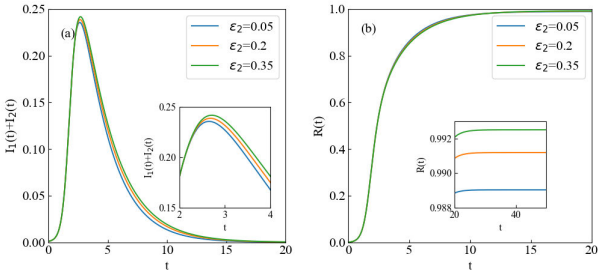

FIGURE 21. Effect of transition probability from not affected area to affected area at second stage on information spreading. (a) The density of two categories of spreaders with the increase of ε_2. (b) The density of recovereds with the increase of ε_2. We set $\alpha_1 = 0.4$, $\alpha_1^{\Delta} = 0.48$, $\beta_1 = 0.3$, $\beta_1^{\Delta} = 0.24$, $\gamma_1 = 0.35$, $\lambda_1 = 0.2$, $\lambda_1^{\Delta} = 0.24$, $\xi_1 = 0.4$, $\xi_1^{\Delta} = 0.32$, $\eta_1 = 0.5$, $\varepsilon_1 = 0.2$, $\delta_1 = \delta_2 = 0.2$, $t_2 = 2$. The blue lines denote the densities of two categories of spreaders and recovereds in each time with $\varepsilon_2 = 0.05$. The orange lines denote the densities of two categories of spreaders and recovereds in each time with $\varepsilon_2 = 0.2$. The green lines denote the densities of two categories of spreaders and recovereds in each time with $\varepsilon_2 = 0.35$.

According to Fig. 20, at the second stage of spatial evolution, assuming the probability that individuals from not affected areas turning into affected areas remains unchanged, if the transition probability from affected areas turning into not affected areas decreases, the maximum densities of the two categories of spreaders and recovereds increase. On the contrary, if the transition probability from affected areas turning into not affected areas increases, the maximum densities of the two categories of spreaders and recovereds decrease. Contrary to this result, as shown in Fig. 21, at the second stage of spatial evolution, assuming the probability that individuals from affected areas turning into not affected areas remains unchanged, if the transition probability from not affected areas turning into affected areas decreases, the maximum densities of the two categories of spreaders and recovereds decrease. On the contrary, if the transition probability from not affected areas turning into affected areas increases, the maximum densities of the two categories of spreaders and recovereds increase. In addition, the numerical simulations results in Fig. 20-Fig. 21 also show that the maximum densities of the two categories of spreaders and recovereds decrease as the probability of the individual turning from affected areas to not affected areas increases and the probability of the individuals turning from not affected areas to affected areas decreases. The above results show that the spatial deterioration would accelerate the spread of public health emergency information, and further aggravate the negative effect of information.

3) EFFECT OF THE SPATIAL EVOLUTION TIME OF PUBLIC HEALTH EMERGENCY

In order to further analyze the effect of spatial evolution time on the information spreading, the densities' changes of the two categories of spreaders and recovereds under different spatial evolution trends and evolution time are explored without considering local evolution in affected areas. Obviously, if the probability that individuals turn from affected areas to not affected area decreases, and the probability that individuals turn from not affected areas to affected areas increases, the public health emergency gets worse in space. On the contrary, if the probability that individuals turn from affected areas to not affected areas increases, and the probability that individuals turn from not affected areas to affected areas decreases, the public health emergency gets better in space.

As can be seen from Fig. 22, the earlier the spatial deterioration evolution, the greater the maximum densities of the two categories of spreaders and recoveoreds. By contrast, as can be seen from Fig. 23, the earlier the spatial improvement, the smaller the maximum densities of the two categories of spreaders and recovereds. These results show that the wider the coverage of affected areas, the faster and the wider the spread of public health emergency information. On the contrary, the smaller the coverage areas of affected areas, the slower the spread of public health emergency information, and the smaller the spreading scale. Besides, the spatial deterioration of public health emergency is related to the movement of individuals closely. Therefore, we should

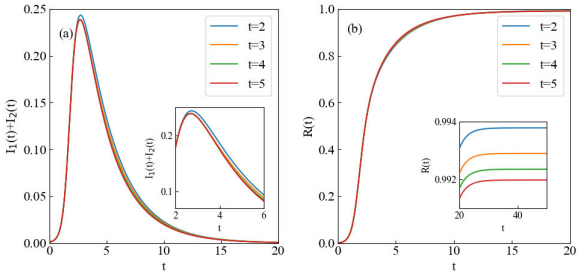

FIGURE 22. Effect of spatial deterioration time of public health emergency on information spreading. (a) The density of two categories of spreaders with the increase of t_2. (b) The density of recovereds with the increase of t_2. We set $\alpha_1 = 0.4$, $\alpha_1^{\Delta} = 0.48$, $\beta_1 = 0.3$, $\beta_1^{\Delta} = 0.24$, $\gamma_1 = 0.35$, $\lambda_1 = 0.2$, $\lambda_1^{\Delta} = 0.24$, $\xi_1 = 0.4$, $\xi_1^{\Delta} = 0.32$, $\eta_1 = 0.5$, $\delta_1 = \varepsilon_1 = 0.2$, $\delta_2 = 0.05$, $\varepsilon_2 = 0.35$. The blue lines denote the densities of two categories of spreaders and recovereds in each time with $t_2 = 2$. The orange lines denote the densities of two categories of spreaders and recovereds in each time with $t_2 = 3$. The green lines denote the densities of two categories of spreaders and recovereds in each time with $t_2 = 4$. The red lines denote the densities of two categories of spreaders and recovereds in each time with $t_2 = 5$.

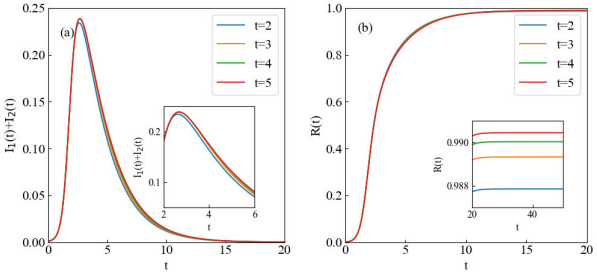

FIGURE 23. Effect of spatial improvement time of public health emergency on information spreading. (a) The density of two categories of spreaders with the increase of t_2. (b) The density of recovereds with the increase of t_2. We set $\alpha_1 = 0.4$, $\alpha_1^{\Delta} = 0.48$, $\beta_1 = 0.3$, $\beta_1^{\Delta} = 0.24$, $\gamma_1 = 0.35$, $\lambda_1 = 0.2$, $\lambda_1^{\Delta} = 0.24$, $\xi_1 = 0.4$, $\xi_1^{\Delta} = 0.32$, $\eta_1 = 0.5$, $\delta_1 = \varepsilon_1 = 0.2$, $\delta_2 = 0.35$, $\varepsilon_2 = 0.05$. The blue lines denote the densities of two categories of spreaders and recovereds in each time with $t_2 = 2$. The orange lines denote the densities of two categories of spreaders and recovereds in each time with $t_2 = 3$. The green lines denote the densities of two categories of spreaders and recovereds in each time with $t_2 = 4$. The red lines denote the densities of two categories of spreaders and recovereds in each time with $t_2 = 5$.

pay attention to the movement of individuals in affected areas as soon as possible to control the spreading of public health emergency information.

V. CONCLUSION

In summary, we propose a novel $S_1S_2I_1I_2R$ multi-stage information spreading dynamic model in simplicial complexes considering the spatiotemporal evolution effect of public health emergency. In the novel model, not only pairwise interactions are analyzed, but the group interactions are also studied, which is discussed by taking 2-simplex as an example. Then the mean-field state transition equations are derived driven by the spatiotemporal evolution under public health emergency, and the basic reproduction number is estimated, too. The results of numerical simulations and real data experiments are found to be matched well. Furthermore, extensive numerical simulations are conducted to reveal the information spreading law.

Through the extensive experiments, the key new results are as follows. Firstly, the strength effect of group interactions in simplicial complexes would increase possibility of individuals spreading information. This would result that the information's maximum impact might be expanded, and the spreading scale might be enlarged. Secondly, the initial impact of public health emergency has a strong promotion effect on the information spreading. Thirdly, the local and spatial deterioration of public health emergency would lead to the rapid spread, and the greater and the earlier the deterioration, the faster the spread of the information. Especially, as the local deterioration occurs after the information spreading slowing down, there would be a rebound phenomenon, and the new peak would be negative correlated with the initial impact of the public health emergency. At last, with the public health emergency in different regions getting worse or better in succession, the information's maximum impact and the spreading scale would be also enlarged. These results suggest that the government should do a good job in monitoring and early warning of public health emergency through multiple channels, and activate the emergency command system immediately to reduce the negative impact of the public health emergency.

In recent years, a variety of public health emergencies occur frequently and present some special characteristics such as sudden, high-intensity, long-period, cross-regional evolution and so on. This leads to the large-scale spreading of public health emergency information which springs up with multi stages and peaks. Besides, the relevant information could spread through different ways, such as the pairwise interactions and group interactions based on simplicial complexes. We provide a new idea to extend the information spreading process to a high-order network structure, and construct multi-stage information spreading model with the spatiotemporal evolution effect of public health emergency. The current results are really inspiring for government to device prevention and control strategies according to the evolution of the public health emergency to deal with public health information which have serious impact on society. In the future, we may apply other high-order structures into the public health emergency information spreading process and study the immunization strategy in further.

DATA AVAILABILITY

Data and code will be made available on request.

REFERENCES

[1] P. Wang, H. Shi, X. Wu, and L. Jiao, "Sentiment analysis of rumor spread amid COVID-19: Based on Weibo text," *Healthcare*, vol. 9, no. 10, p. 1275, Sep. 2021.

[2] Q. Sun, Z. Wang, D. Zhao, C. Xia, and M. Perc, "Diffusion of resources and their impact on epidemic spreading in multilayer networks with simplicial complexes," *Chaos, Solitons Fractals*, vol. 164, Nov. 2022, Art. no. 112734.

[3] P. Luo, C. Wang, F. Guo, and L. Luo, "Factors affecting individual online rumor sharing behavior in the COVID-19 pandemic," *Comput. Hum. Behav.*, vol. 125, Dec. 2021, Art. no. 106968.

[4] X. Liu, S. Cao, L. Zheng, F. Gong, X. Wang, and J. Zhou, "POCA4SD: A public opinion cellular automata for situation deduction," *IEEE Trans. Computat. Social Syst.*, vol. 8, no. 1, pp. 201–213, Feb. 2021.

[5] K. Zhao, "Probing the oscillatory behavior of Internet game addiction via diffusion PDE model," *Axioms*, vol. 11, no. 11, p. 649, Nov. 2022.

[6] K. Zhao, "Global stability of a novel nonlinear diffusion online game addiction model with unsustainable control," *AIMS Math.*, vol. 7, no. 12, pp. 20752–20766, 2022.

[7] A. Cichocka, "To counter conspiracy theories, boost well-being," *Nature*, vol. 587, no. 7833, p. 177, Nov. 2020.

[8] Y. Zhang, Y. Su, L. Weigang, and H. Liu, "Rumor and authoritative information propagation model considering super spreading in complex social networks," *Phys. A, Stat. Mech. Appl.*, vol. 506, pp. 395–411, Sep. 2018.

[9] E. Amin, L. Socheanet, and P. Meel, "Enhancing the detection of fake news in social media based on machine learning models," in *Proc. 2nd Int. Conf. Appl. Artif. Intell. Comput. (ICAAIC)*, Salem, India, May 2023, pp. 305–312.

[10] F. A. Ozbay and B. Alatas, "Fake news detection within online social media using supervised artificial intelligence algorithms," *Phys. A, Stat. Mech. Appl.*, vol. 540, Feb. 2020, Art. no. 123174.

[11] K. Zhao, "Attractor of a nonlinear hybrid reaction-diffusion model of neuroendocrine transdifferentiation of human prostate cancer cells with time-lags," *AIMS Math.*, vol. 8, no. 6, pp. 14426–14448, 2023.

[12] W. O. Kermack and A. G. McKendrick, "A contribution to the mathematical theory of epidemics," *Proc. Roy. Soc. London. Ser. A, Containing Papers Math. Phys. Character*, vol. 115, no. 772, pp. 700–721, Aug. 1927.

[13] D. J. Daley and D. G. Kendall, "Stochastic rumours," *IMA J. Appl. Math.*, vol. 1, no. 1, pp. 42–55, Mar. 1965.

[14] D. P. Maki and M. Thompson, *Mathematical Models and Applications*. Upper Saddle River, NJ, USA: Prentice-Hall, 1973.

[15] K. Zhao, "Existence and stability of a nonlinear distributed delayed periodic AG-ecosystem with competition on time scales," *Axioms*, vol. 12, no. 3, p. 315, Mar. 2023.

[16] K. Zhao, "Local exponential stability of several almost periodic positive solutions for a classical controlled GA-predation ecosystem possessed distributed delays," *Appl. Math. Comput.*, vol. 437, Jan. 2023, Art. no. 127540.

[17] J. Fumanal-Idocin, O. Cordón, G. P. Dimuro, A. R. López-de-Hierro, and H. Bustince, "Quantifying external information in social network analysis: An application to comparative mythology," *IEEE Trans. Cybern.*, early access, Feb. 10, 2023, doi: 10.1109/TCYB.2023.3239555.

[18] D. J. Watts and S. H. Strogatz, "Collective dynamics of 'small-world' networks," *Nature*, vol. 393, no. 6684, p. 440, Jun. 1998.

[19] A.-L. Barabási and R. Albert, "Emergence of scaling in random networks," *Science*, vol. 286, no. 5439, pp. 509–512, Oct. 1999.

[20] D. H. Zanette, "Dynamics of rumor propagation on small-world networks," *Phys. Rev. E, Stat. Phys. Plasmas Fluids Relat. Interdiscip. Top.*, vol. 65, no. 4, Mar. 2002, Art. no. 041908.

[21] Y. Moreno, R. Pastor-Satorras, and A. Vespignani, "Epidemic outbreaks in complex heterogeneous networks," *Eur. Phys. J. B Condens. Matter Complex Syst.*, vol. 26, no. 4, pp. 521–529, Apr. 2002.

[22] M. Nekovee, Y. Moreno, G. Bianconi, and M. Marsili, "Theory of rumour spreading in complex social networks," *Phys. A, Stat. Mech. Appl.*, vol. 374, no. 1, pp. 457–470, Jan. 2007.

[23] L. Zhang, C. Su, Y. Jin, M. Goh, and Z. Wu, "Cross-network dissemination model of public opinion in coupled networks," *Inf. Sci.*, vols. 451–452, pp. 240–252, Jul. 2018.

[24] Y. Chai, Y. Wang, and L. Zhu, "A stochastic information diffusion model in complex social networks," *IEEE Access*, vol. 7, pp. 175897–175906, 2019.

[25] Y. Dong, L. Huo, and L. Zhao, "An improved two-layer model for rumor propagation considering time delay and event-triggered impulsive control strategy," *Chaos, Solitons Fractals*, vol. 164, Nov. 2022, Art. no. 112711.

[26] Q. Han, K. Shi, M. Gu, L. You, and F. Miao, "Modeling repeated rumor spreading in coupled social networks," *IEEE Access*, vol. 9, pp. 89732–89740, 2021.

[27] W. Jing, Y. Li, X. Zhang, J. Zhang, and Z. Jin, "A rumor spreading pairwise model on weighted networks," *Phys. A, Stat. Mech. Appl.*, vol. 585, Jan. 2022, Art. no. 126451.

[28] Q. Shao, C. Xia, L. Wang, and H. Li, "A new propagation model coupling the offline and online social networks," *Nonlinear Dyn.*, vol. 98, no. 3, pp. 2171–2183, Nov. 2019.

[29] H. Zhao, X. Liu, and Y. Wang, "Tripartite evolutionary game analysis for rumor spreading on Weibo based on MA-PT," *IEEE Access*, vol. 9, pp. 90043–90060, 2021.

[30] L. Zhu and L. He, "Two different approaches for parameter identification in a spatial–temporal rumor propagation model based on Turing patterns," *Commun. Nonlinear Sci. Numer. Simul.*, vol. 107, Apr. 2022, Art. no. 106174.

[31] S. Ai, S. Hong, X. Zheng, Y. Wang, and X. Liu, "CSRT rumor spreading model based on complex network," *Int. J. Intell. Syst.*, vol. 36, no. 5, pp. 1903–1913, May 2021.

[32] Y. Cheng, L. Huo, and L. Zhao, "Dynamical behaviors and control measures of rumor-spreading model in consideration of the infected media and time delay," *Inf. Sci.*, vol. 564, pp. 237–253, Jul. 2021.

[33] X. Wang, Y. Li, J. Li, Y. Liu, and C. Qiu, "A rumor reversal model of online health information during the COVID-19 epidemic," *Inf. Process. Manage.*, vol. 58, no. 6, Nov. 2021, Art. no. 102731.

[34] Q. Suo, J.-L. Guo, and A.-Z. Shen, "Information spreading dynamics in hypernetworks," *Phys. A, Stat. Mech. Appl.*, vol. 495, pp. 475–487, Apr. 2018.

[35] F. Yin, J. Lv, X. Zhang, X. Xia, and J. Wu, "COVID-19 information propagation dynamics in the Chinese Sina-microblog," *Math. Biosci. Eng.*, vol. 17, no. 3, pp. 2676–2692, 2020.

[36] Z. Wang, J. Liang, H. Nie, and H. Zhao, "A 3SI3R model for the propagation of two rumors with mutual promotion," *Adv. Difference Equ.*, vol. 2020, no. 1, p. 109, Mar. 2020.

[37] W. Liu, X. Wu, W. Yang, X. Zhu, and S. Zhong, "Modeling cyber rumor spreading over mobile social networks: A compartment approach," *Appl. Math. Comput.*, vol. 343, pp. 214–229, Feb. 2019.

[38] F. Yin, X. Jiang, X. Qian, X. Xia, Y. Pan, and J. Wu, "Modeling and quantifying the influence of rumor and counter-rumor on information propagation dynamics," *Chaos, Solitons Fractals*, vol. 162, Sep. 2022, Art. no. 112392.

[39] Y. Zhang and J. Xu, "A dynamic competition and predation model for rumor and rumor-refutation," *IEEE Access*, vol. 9, pp. 9117–9129, 2021.

[40] J. Zhao, H. He, X. Zhao, and J. Lin, "Modeling and simulation of microblog-based public health emergency-associated public opinion communication," *Inf. Process. Manage.*, vol. 59, no. 2, Mar. 2022, Art. no. 102846.

[41] R. Li, Y. Li, Z. Meng, Y. Song, and G. Jiang, "Rumor spreading model considering individual activity and refutation mechanism simultaneously," *IEEE Access*, vol. 8, pp. 63065–63076, 2020.

[42] U. Alvarez-Rodriguez, F. Battiston, G. F. de Arruda, Y. Moreno, M. Perc, and V. Latora, "Evolutionary dynamics of higher-order interactions in social networks," *Nature Human Behaviour*, vol. 5, no. 5, pp. 586–595, Jan. 2021.

[43] M. Jusup, P. Holme, K. Kanazawa, M. Takayasu, I. Romic, Z. Wang, S. Gecek, T. Lipic, B. Podobnik, L. Wang, W. Luo, T. Klanjscek, J. Fan, S. Boccaletti, and M. Perc, "Social physics," *Phys. Rep.*, vol. 948, pp. 1–148, Feb. 2022.

[44] N. W. Landry and J. G. Restrepo, "The effect of heterogeneity on hypergraph contagion models," *Chaos, Interdiscipl. J. Nonlinear Sci.*, vol. 30, no. 10, Oct. 2020, Art. no. 103117.

[45] J. Fan, Q. Yin, C. Xia, and M. Perc, "Epidemics on multilayer simplicial complexes," *Proc. Roy. Soc. A, Math., Phys. Eng. Sci.*, vol. 478, no. 2261, May 2022, Art. no. 20220059.

[46] J. T. Matamalas, S. Gómez, and A. Arenas, "Abrupt phase transition of epidemic spreading in simplicial complexes," *Phys. Rev. Res.*, vol. 2, no. 1, Feb. 2020, Art. no. 012049.

[47] Z. Li, Z. Deng, Z. Han, K. Alfaro-Bittner, B. Barzel, and S. Boccaletti, "Contagion in simplicial complexes," *Chaos, Solitons Fractals*, vol. 152, Nov. 2021, Art. no. 111307.

[48] S. Gao, L. Chang, M. Perc, and Z. Wang, "Turing patterns in simplicial complexes," *Phys. Rev. E, Stat. Phys. Plasmas Fluids Relat. Interdiscip. Top.*, vol. 107, no. 1, Jan. 2023, Art. no. 014216.

[49] I. Iacopini, G. Petri, A. Barrat, and V. Latora, "Simplicial models of social contagion," *Nature Commun.*, vol. 10, no. 1, p. 2485, Jun. 2019.

[50] B. Jhun, "Effective epidemic containment strategy in hypergraphs," *Phys. Rev. Res.*, vol. 3, no. 3, Sep. 2021, Art. no. 033282.
[51] F. P. Morgeson, T. R. Mitchell, and D. Liu, "Event system theory: An event-oriented approach to the organizational sciences," *Acad. Manage. Rev.*, vol. 40, no. 4, pp. 515–537, Oct. 2015.
[52] P. Ning, P. Cheng, J. Li, M. Zheng, D. C. Schwebel, Y. Yang, P. Lu, M. Li, Z. Zhang, and G. Hu, "COVID-19-related rumor content, transmission, and clarification strategies in China: Descriptive study," *J. Med. Internet Res.*, vol. 23, no. 12, Dec. 2021, Art. no. e27339.
[53] B. Zhu, X. Zheng, H. Liu, J. Li, and P. Wang, "Analysis of spatiotemporal characteristics of big data on social media sentiment with COVID-19 epidemic topics," *Chaos, Solitons Fractals*, vol. 140, Nov. 2020, Art. no. 110123.
[54] L. Huo and X. Xie, "Dynamical analysis of dual product information diffusion considering preference in complex networks," *Complexity*, vol. 2020, Apr. 2020, Art. no. 6819512.
[55] L. Lü, D.-B. Chen, and T. Zhou, "The small world yields the most effective information spreading," *New J. Phys.*, vol. 13, no. 12, Dec. 2011, Art. no. 123005.
[56] Y. Zhang, Y. Su, L. Weigang, and H. Liu, "Interacting model of rumor propagation and behavior spreading in multiplex networks," *Chaos, Solitons Fractals*, vol. 121, pp. 168–177, Apr. 2019.
[57] J. Gómez-Gardeñes, V. Latora, Y. Moreno, and E. Profumo, "Spreading of sexually transmitted diseases in heterosexual populations," *Proc. Nat. Acad. Sci. USA*, vol. 105, no. 5, pp. 1399–1404, Feb. 2008.
[58] Y. Zan, J. Wu, P. Li, and Q. Yu, "SICR rumor spreading model in complex networks: Counterattack and self-resistance," *Phys. A, Stat. Mech. Appl.*, vol. 405, pp. 159–170, Jul. 2014.
[59] Y. Zhang and Y. Feng, "Two-layer coupled network model for topic derivation in public opinion propagation," *China Commun.*, vol. 17, no. 3, pp. 176–187, Mar. 2020.
[60] L. Qian, "Making memory work: The SARS memory and China's war on COVID-19," *Memory Stud.*, vol. 14, no. 6, pp. 1489–1502, Dec. 2021.

YANYUAN SU received the Ph.D. degree from Yanshan University, Qinhuangdao, China, in 2019. She is currently an Associate Professor with the School of Economics and Management, Yanshan University. Her research interests include complex networks, social networks, information spreading, and spreading dynamics.

YAMING ZHANG received the Ph.D. degree from Renmin University, Beijing, China, in 2002. He is currently a Professor and the Ph.D. Supervisor with the School of Economics and Management, Yanshan University, Qinhuangdao, China, where he is also the Director of the Research Center of Internet Plus and Industry Development. He has been a principal investigator/a co-investigator on several research projects, supported by the National Natural Science Foundation of China, the National Social Science Foundation of China, and other foundations. He is the (co)author of more than 200 articles in technique and management journals. His research interests include complex networks and spreading dynamics.

LI WEIGANG (Senior Member, IEEE) received the Ph.D. degree from the Aeronautics Institute of Technology (ITA), Brazil, in 1994. He is a Professor and the Director of the Transportation Intelligent Computing Laboratory (TransLab), Department of Computer Science (CIC), University of Brasilia (UnB), Brazil. He has coordinated various research and development projects, supported by some promotion foundations and also the industry partners, such as Atech, Boeing, CAPES, CNPq, FAPDF, and FINEP. He advised more than 120 students, including bachelor's, master's, and Ph.D. students and postdoctoral researchers. His research direction related to artificial intelligence and machine learning in intelligent transportation, social networks, natural language processing, and others.